Green manuring increased peanut yields and reduced soil carbon mineralization by optimizing microbial communities

Qiqi Sun

sunshine19890707@163.com

Shandong Peanut Research Institute https://orcid.org/0000-0002-2672-319X

Yongmei Zheng
Xuewu Sun
Lijun Wu
Zhengfeng Wu
Jialei Zhang
Tianyi Yu
Shubo Wan
Jiancheng Zhang

Research Article

Keywords: peanut, green manure, microbial communities, soil organic carbon mineralization

Posted Date: November 30th, 2023

DOI: https://doi.org/10.21203/rs.3.rs-3640713/v1

Version of Record: A version of this preprint was published at Plant and Soil on September 30th, 2024.
See the published version at https://doi.org/10.1007/s11104-024-06965-4.

Abstract

Using green manure (GM) in rotations is a sustainable approach to cleaner production and soil CO_2 emissions mitigation, yet the microbial mechanism governing soil organic carbon (SOC) mineralization from legume fields remains to be elucidated. To determine whether the GM-based rotation was superior to the conventional continuous peanut monoculture, a seven-year field experiment including two cropping regimes, peanut continuous monoculture (P) and peanut-*Orychophragmus violaceus* rotation (PO), was performed. Microbial properties and C-degradation enzyme activities in the rhizosphere and bulk soil of peanut fields were explored, with SOC mineralization (K_c) and its temperature sensitivity (Q_{10}) determined in the laboratory. *O. violaceus* incorporation as a GM enhanced soil moisture, pH and mineral nitrogen contents, which increased the bulk soil bacterial alpha diversity and reduced rhizosphere fungal richness. GM incorporation promoted saprotrophs (Agaricales), enriched beneficial microbes (Bacillus) and inhibited pathogenic fungi (*Fusarium*), thus alleviating continuous monoculture obstacles and increasing yields. The bacterial interaction complexity was increased, but the fungal interaction complexity was reduced. Moreover, GM not only decreased the rhizosphere Q_{10} (by 14.9%) due to decreased rhizosphere SOC but also reduced the bulk soil K_c (by 23.9%) due to the intensified C limitation, indicating that the C loss of bulk soil is currently low and that of the rhizosphere will be limited under future warming. This study provides new insight into soil C mineralization in legumes at the microenvironmental scale, and improves our projections of legume soil C loss under future climate change scenarios.

1. Introduction

Current agricultural development requires equal emphasis on high yields and low carbon emissions (Mueller et al. 2012). Green manuring is a multiple ecological service agricultural practice used to facilitate the growth of subsequent cash crops (Liang et al. 2023). Evidence suggests that green manure (GM)-based rotations may enhance SOC sequestration and mitigate greenhouse gas emissions in agroecosystems (Forte et al. 2017; Ho et al. 2021), thereby contributing to ‘carbon neutralization’ (Li et al. 2022). However, our understanding of the effect of GM-rotation on the agricultural soil organic carbon (SOC) dynamics lags significantly behind that of other farming practices. Researchers have found that GM inclusion-induced changes in SOC mineralization (K_c) remain a debatable topic. The positive effect of GM incorporation on soil C mineralization of succeeding crops has been reported, such as in a short-term winter cover crop/sweet pepper rotation in a Mediterranean environment (Mancinelli et al. 2013), in a 100-day experiment from paddy soil with coincorporation of rice straw and leguminous GM (Zhou et al. 2020), in a dryland spring maize field on the Loess Plateau of China (Ding et al. 2021), and in a 30-year farmland using maize – wheat intercropping with GM (hairy vetch) amended experiment from an Agricultural Research Station (Bian et al. 2022). In contrast, a negative effect on soil C mineralization has also been reported in typical temperate upland soil (Hwang et al. 2020) and in a two-year GM-maize field system in upland soil (Ho et al. 2021). In addition, neutral responses of C mineralization have also been reported in Mediterranean drip irrigated maize production systems (Forte et al. 2017). These discrepant

findings may be related to the initial N status of the soil (Yim et al. 2022), which differs in legume and nonlegume ecosystems, and to varying GM crops (Ho et al. 2021). The residue with a carbon to nitrogen ratio (C/N) of 25 is the best option because of lower net global warming potential (Zhou et al. 2020). In the soil of the nonleguminous field, GM with a low C/N ratio accelerates C mineralization by supplying labile C and N and promoting *r*-strategists (Bian et al. 2022), while GM with a higher C/N ratio will constrain microbial decomposition of crop straw due to N immobilization (Zhou et al. 2020). Nevertheless, contrasting responses likely occurred in the soil of the legume field. Therefore, the effect of GM incorporation on soil C mineralization may be related to the changes in soil C and N availability and different C/N ratios of incorporated crops. In addition, the interaction between soil and crop residues (priming effect) also affects microbial decomposition (Kuzyakov et al. 2000). Scientists have researched the priority of legume incorporation as GM to nonlegume in benefiting arable soil (Yan et al. 2023b), yet few have paid attention to soil C mineralization and CO_2 emission of the legume field that inherently had a low soil C/N ratio, especially under GM incorporation.

The process of SOC mineralization is driven by soil microorganisms, which determine the key feedback between soil and climate in response to the fresh carbon input (Liu et al. 2018b). Rhizosphere and bulk soil have distinct physicochemical (Tringe et al. 2005) and microbial (Zhang et al. 2017) properties due to the existence of root exudates and root selection processes. As a ubiquitous disturbance to arable soil that amends fresh organic residues, green manuring can reshape the composition of soil and root-associated microbes (Liang et al. 2023), which mediate the residual decomposition process of cultivated crops after being pressed into soil, and directly change SOC mineralization (Muhammad et al. 2022). For example, 31 years of rice-rice-GM rotations increased the bacterial abundance and enriched the plant-growth-promoting rhizobacteria *Acinetobacter* and *Pseudomonas*, while no significant difference in the bulk soil was observed (Zhang et al. 2017), suggesting that the rhizosphere microbial community could be more sensitive to plant and soil nutrient changes. Furthermore, different sizes of soil aggregates create a composite of ecological niches differing in terms of physico-chemical and structural characteristics supporting distinct microbial assemblages (Li et al. 2023), and these variations are major factors affecting SOC mineralization. Knowledge of microbial communities within different aggregates is essential for understanding the mechanisms underlying soil microbe-driven changes in soil C mineralization. Therefore, clarifying the mechanisms of microbial regulation of soil C mineralization and its temperature sensitivity (expressed as Q_{10} (Xu and Qi 2001)) at the soil microenvironmental scale (at bulk and aggregate levels) provides insights into microbial mechanisms that regulate carbon sequestration and emission reduction of arable soil and improve cultivated land quality, especially under the conditions of food security and climate change.

The peanut (*Arachis hypogaea L.*) is the fourth largest oilseed in the world, showing significant potential for decreasing C emissions from agricultural production activity (He et al. 2021). Against the backdrop of China's higher external dependence on oil demand, peanuts are a good substitute for soybeans (Wan et al. 2010; Yan et al. 2023a); thus, the Chinese peanut area will probably increase in the following years. Therefore, it is necessary to quantify SOC mineralization in peanut cropping to reduce the potential

environmental impacts of the agricultural sector (He et al. 2021). Crop rotations with a legume could theoretically increase SOC sequestration compared with those without a legume (Trivedi et al. 2015). Nevertheless, in the case of peanuts, straw is annually removed as a high-quality feedstuff instead of being returned to the field in China, which is not conducive to SOC sequestration (Zhao et al. 2017). In addition, peanut yields and farmland quality have long been seriously compromised by continuous cropping obstacles, which probably led to a decrease in soil quality (Wu et al. 2023a). Peanut rotation with GM (e.g., oilseed rape) has been proposed as an effective strategy to overcome continuous cropping obstacles (Xu et al. 2023), with the concern of additional production of more CO_2 emissions. To reduce C loss and improve the quality of arable land, a new alternative winter GM-peanut planting system was established, in which *Orychophragmus violaceus L*. (*O. violaceus*) was used as the GM crop. *O. violaceus* (Cruciferae, one of the common GM crops, C/N < 25) is a new GM crop on the North China Plain with advantages in reducing greenhouse gas emissions and increasing net ecosystem economic benefits (Zhang et al. 2021). Therefore, it is imperative to generate a better understanding of the responses of rhizosphere and bulk soil microbial ecology of peanut fields to the incorporation of *O. violaceus* as a GM.

To bridge this knowledge gap, we provide a comprehensive comparison and exploration of the effects of continuous and rotational peanut cropping on soil-peanut ecology (peanut yield, rhizosphere and bulk soil microbial community structure and function, rhizosphere and bulk soil physicochemical properties), SOC mineralization (K_c) and its temperature sensitivity (Q_{10}), as well as their correlations. Moreover, the bulk soil microbial communities, enzyme activities, K_c, Q_{10} and functional genes were determined at the aggregate scale. It was hypothesized that: 1) GM inclusion would simultaneously improve peanut yield and reduce SOC mineralization by optimizing soil microbial communities and 2) the rhizosphere and bulk soil would have contrasting responses to GM incorporation in terms of microbial communities and SOC mineralization.

2. Materials and methods

2.1. Experimental design and soil sampling

The study site was in the Laixi experimental station of Shandong Peanut Research Institute, Shandong Province, China (36°48'47"N, 120°30'17"E). The Laixi experimental station experiences a semihumid monsoon climate, with a mean annual rainfall of 732 mm and a daily air temperature of 11.3 ℃. The soil at the experimental site is categorized as brown soil (Haplic Luvisol, FAO Soil Taxonomy System). At the beginning of the experiment in September 2017, the soil at 0 − 20 cm depth had a pH of 5.38, soil organic matter of 12.05 g kg^{-1}, available nitrogen of 75.6 mg kg^{-1}, available phosphorus of 27.92 mg kg^{-1} and available potassium of 192 mg kg^{-1}. Two planting modes, peanut continuous monoculture (P) and peanut-*O. violaceus* rotation (PO), were established, with a randomized block design in triplicate. The size of each experimental plot was 20 m×5 m. The peanut variety Huayu 22 was planted in May in ridges and furrows under plastic film mulching, with two seeds sown in each hole. Compound fertilizers

($N:P_2O_5:K_2O$ = 15:15:15) were applied before seeding at 750 kg ha^{-1}. During the experimental period, the highly nutritious peanut straw was annually removed as feedstuff after harvest. *O. violaceus* and peanut have been rotated annually since 2017 in the PO treatment. *O. violaceus* was planted in October and harvested in April, and the seeding rate was approximately 45 t seeds ha^{-1} to ensure at least 8 billion emergence. The fresh biomass of *O. violaceus* during the blooming stage was chopped into small fragments (2 ~ 3 cm) and returned to the field to a depth of approximately 25 cm before peanut transplantation (NPK + *O. violaceus*), with an incorporation rate of approximately 45 t ha^{-1}. At the return time, the water content of *O. violaceus* was 88.8%, and the nitrogen, phosphorus, potassium and carbon contents in the biomass were 39.2, 4.2, 28.4 and 381.7 g kg^{-1}, respectively.

At the maturing stage of the peanuts in 2023, three composite soil samples at each treatment of P and PO were taken as the bulk soil (B). Each composite soil sample consisted of five subsamples collected randomly from 0 – 20 cm topsoil, with a 2.5 cm diameter auger from each plot. Furthermore, three complete peanut plants for each plot were taken out with their immediate block of soil included. The soil tightly adhering to the roots was gathered as rhizosphere soil (R). Each composite soil sample was then passed through an 8.0-mm sieve and divided into three parts: One part was stored at − 80°C for DNA extraction; the second part was stored at 4°C for measurements of SOC mineralization rate (K_c), soil nitrate (NO_3^--N) and ammonium (NH_4^+-N) nitrogen, soil dissolved organic carbon (DOC), microbial biomass carbon (MBC) and activities of soil carbon-degradation enzymes; and the third part was air-dried to determine SOC, soil total nitrogen (TN) and soil pH. In addition, to investigate the aggregate size distribution, approximately 1000 g of undisturbed bulk soil was randomly collected from the upper 15 cm of each treatment using a cylindrical metal core (10 cm in diameter).

2.2. High-throughput sequencing and bioinformatics analysis

Soil DNA was extracted using an E.Z.N.A.® soil DNA kit (Omega Biotek, Norcross, GA, U.S.). The DNA was quantified and qualified with a NanoDrop-2000 instrument and was used as a PCR template. The bacterial 16S rRNA gene fragments (V3-V4 region) were amplified using the primers 338F (5'-ACTCCTACGGGAGGCAGCAG-3') and 806R (5'-GGACTACHVGGGTWTCTAAT-3'), and fungal ITS1 genes were amplified using primers 1737F (5'-TCCGTAGGTGAACCTGCGG-3') and 2043R (5'-GCTGCGTTCTTCATCGATGC-3') (Caporaso et al. 2011). The PCR products were paired-end sequenced using the MiSeq PE300 platform (Illumina, San Diego, CA, USA) provided by the Illumina Corporation.

Raw sequences were processed with QIIME, and chimeras were detected using UCHIME (Magoč and Salzberg 2011). After quality filtering and removal of chimeric sequences, all remaining high-quality sequences were clustered into operational taxonomic units (OTUs) at 97% similarity using Usearch software (version 7.0 http://drive5.com/uparse/). Taxonomic assignment was conducted using the RDP classifier (http://rdp.cme.msu.edu/) after comparison of each read to the SILVA database (SSU132), with a threshold of 70%. Sequence analysis was performed by the UPARSE software package using the UPARSE-OTU and UPARSE-OTUref algorithms (Edgar 2013). Alpha-diversity indices, including the Chao1

estimator of richness and Shannon's diversity index were generated based on the obtained OTUs. The ecological functions of the bacterial and fungal communities were predicted by the FARPROTAX (v1.1) and FUNGuild databases.

2.3. SOC mineralization rate (K_c) and Q_{10}

Fifty grams of fresh soil was placed into a 500-ml butyl lithium bottle and incubated at six temperature gradients: 5°C, 10°C, 15°C, 20°C, 25°C and 30°C to systematically measure the SOC mineralization rate. The incubation method has been previously described (Ding et al. 2017; Lefèvre et al. 2014) and verified in our previous study (Wu et al. 2023a). After being preincubated, 50 grams of fresh samples were placed into the butyl lithium bottle, accompanied by three plastic bottles containing NaOH liquid to absorb the released CO_2 and three plastic bottles containing NaOH liquid with no soil sample to calculate the CO_2 absorbed from air. All the bottles were incubated, firstly at 5°C for 48 h, then at 10°C, 15°C, 20°C and 25°C for 24 h consecutively, and finally at 30°C for 12 h. The CO_2 concentration in each bottle was measured by the alkali absorption method. The K_c of each sample was calculated by the differences in CO_2 concentration over a certain period per unit of dry weight.

The relationship between temperature and K_c is described as follows (Davidson et al. 1998; Xu and Qi 2001):

$$K_c = ae^{\beta T}$$

$$Q_{10} = e^{10\beta}$$

where K_c is the measured SOC mineralization rate (μg CO_2 g^{-1} dry soil h^{-1}), T is the temperature (°C), and Q_{10} is the temperature sensitivity of SOC mineralization.

2.4. Soil biochemical analysis

The activities of β-1,4-xylosidase (BX), β-1,4-glucosidase (BG) and β-D-cellobiohydrolase (CB) were measured fluorometrically using a 200 μM solution of substrates labeled with 4-methylumbelliferone (MUB), according to the method outlined in Saiya-Cork et al. (2002) and modified by Du et al. (2021). These activities were corrected for quench and negative controls and expressed in units of nmol activity per hour per gram of dry soil (μmol d^{-1} g^{-1}). Together with rhizosphere soil sampling, peanut roots were separated from soils by being soaked in water and gently washed over a 0.25 mm mesh. Nodules on the root were stripped by hand, and then dried with absorbent paper to acquire their fresh weights. Wet roots were oven dried at 60°C for 48 h to a constant weight. At harvest, two representative quadrats (4 m×1 m) were selected for each plot to determine the podding yields.

To obtain the gravimetric moisture content, soil samples were oven-dried at 105°C for 12 h to achieve constant weight. SOC was determined using the K_2CrO_7-H_2SO_4 oxidation method (Dai et al. 2021). TN was measured using the Kjeldahl method (Zeng et al. 2016). The MBC was determined using the

chloroform fumigation-extraction method with a total organic carbon analyzer (TOC-VCSH, Shimadzu, Japan) described in Vance et al. (1987), with a conversion factor of 0.38. The organic carbon in the unfumigated soil extracts was deemed to be DOC. NO_3^--N and NH_4^+-N were extracted with KCl (l mol L^{-1}) and determined by colorimetry using a Bran & Luebbe II AutoAnalyzer. N_{min} was the sum of NO_3^--N and NH_4^+-N, and the soil carbon:nitrogen ratio (C/N) was the ratio of DOC and N_{min}. Soil pH was determined with a digital pH meter (Woonsocket, RI, USA) using a soil-to-water ratio of 1:2.5 (w/v).

2.5. Soil aggregate fractionation

Soil was fractionated using a wet-sieving technique as described in detail by (Davinic et al. 2012) and four fractions were obtained for each sample: Large macroaggregate (> 2 mm), medium macroaggregate (1 − 2 mm), small macroaggregate (0.25 − 1 mm) and microaggregate (< 0.25 mm). DNA extraction, soil properties, K_c and enzyme analyses were performed as described in the previous sections.

2.6. High-throughput qPCR chip analysis

The soil functional gene diversity and composition of each size of soil aggregates were profiled by Guangdong Magigene Technology Co., Ltd using high-throughput qPCR chip technology. We mainly focused on functional genes associated with C-degradation and C-fixation. After DNA extraction, the amount and purity of DNA were tested with a Qubit4.0 instrument (Thermo Fisher Scientific, Waltham, USA) to ensure that the concentrations of DNA were diluted uniformly to 20 ng μL^{-1}. The qualified DNA samples were added to a 384 microplate as a sample source plate, and simultaneously, the primer and reagents used for qPCR were added to another 384 microplate as an assay source plate. The reagents of both the sample source plate and assay source plate were added to the micropores of the high-throughput qPCR chip-SmartChip Mydesign Chip (Takara Biomedical Technology, Clontech) using the high-throughput automatic microsampling device SmartChip Multisample Nanodispenser (Takara Biomedical Technology). The qPCR and fluorescence signal detection were performed in the SmartChip Real-time PCR System (WaferGen Biosystems USA), with the amplification curves and dissolution curves being automatically generated. The Quality control was conducted according to the Ct summary table derived from the Ct values, which were provided by the SmartChip Real-time PCR System. The absolute quantitative information of the 16S rRNA gene was obtained through fluorescence quantitative PCR (Roche, LightCycler 480Ⅱ), and the absolute quantitative information of each target gene in each sample was obtained based on the absolute quantitative transformation of the 16S rRNA gene. The formula is as follows: Relative quantitative of 16S rRNA gene/absolute quantitative of 16S rRNA gene = relative quantitative of the target gene/absolute quantitative of the target gene.

2.7 Statistical analysis

Differences in soil and plant properties, microbial properties, enzyme activities, K_c and Q_{10} values among the four treatments or aggregates (mean ± SD, $n = 3$) were subjected to ANOVA, followed by an LSD test for post hoc comparisons of means, at a significance level of 0.05. Items between the P and PO

treatments (mean ± SD, $n = 3$) were tested by the two independent samples t test, at a significance level of 0.05. Pearson correlation analyses were used to identify the relationship between microbial properties and environmental factors, between microbial properties and K_c and Q_{10}, and between microbial properties and enzyme activities. The statistical analyses were performed using SPSS 20.0 software for Windows (SPSS Inc., Chicago, USA). Principal coordinate analysis (PCoA) and ADONIS analysis at the OTU level were conducted to identify dissimilarity in the microbial community structures in samples. Redundancy analysis at the OTU level was used to identify the most important environmental variables influencing microbial communities. PCoA, ADONIS and redundancy analysis were performed with R software version 4.0.3 with the 'Vegan' package (Team 2012). The figures were generated using Sigmaplot 12.5 software (Systat Software Inc., San Jose, CA, USA).

Linear discriminant analysis effect size (LEfSe) analysis was used to identify the biomarkers among the treatments with a 3.5 threshold. Co-occurrence network analysis was used to explore microbial community interactions for the P and PO treatments. OTUs with an average abundance > 0.1% were selected, and Spearman's correlations of these OTUs with coefficients (ρ) > 0.70 and FDR-adjusted P values < 0.05 were used to construct co-occurrence networks (Casamayor 2012). Network topological features, including modularity, average degree, average path distance, clustering coefficient, average degree and density, were assessed for P and PO networks.

3. Results

3.1. Soil properties and peanut yield

After seven years of rotation, the effect of GM on soil properties was mostly manifested in the improved soil water contents, NO_3^--N contents, N_{min} contents and BG activities in both the rhizosphere and bulk soil (Table 1). In the rhizosphere, soil pH from the P treatment, initially comparable in rhizosphere and bulk soil, was significantly increased with GM; in contrast, SOC, initially and slightly higher in the rhizosphere (11.03 ± 0.52 g kg^{-1}) than in bulk soil, was reduced by 33.0% due to GM incorporation. In the bulk soil, NH_4^+-N, initially comparable in rhizosphere and bulk soil, was greatly increased by 140.3% with GM inclusion. BX activities varied little among treatments, while the CB activity, initially 27.7% higher in rhizosphere vs. bulk soil, was significantly decreased by 34.9% in the rhizosphere with GM incorporation (Table 1). As expected, GM inclusion positively affected on peanut yields. Three years of data (2021 – 2022) indicated that podding yields were 19.4% ($P < 0.05$), 194.3% ($P < 0.05$) and 33.5% ($P < 0.05$) higher in PO than in P in 2021, 2022 and 2023, respectively (Fig. 1a), with the average being slightly higher (by 51.9%, $P > 0.05$) in PO vs. P (3070.4 ± 861.4 kg ha^{-1}). The root biomass under the PO treatment was slightly lower than that under the P treatment (7.09 ± 0.92 g $plant^{-1}$, Fig. 1b), partly due to the greater soil water content. In contrast, the fresh weight of nodules was 4.4 times higher ($P < 0.05$) under the PO treatment than under the P treatment, suggesting the promotion of nitrogen fixation by nodules (Fig. 1c).

Table 1
Soil physicochemical and biological properties sampled in the maturing stage, 2023

Items [a]	P		PO	
	R	B	R	B
Soil bulk density/g cm^{-3}	—	1.39 ± 0.06a	—	1.46 ± 0.02a
Water content/%	13.36 ± 0.16b	13.32 ± 0.62b	15.55 ± 0.31a	14.95 ± 0.49a
pH	5.39 ± 0.01b	5.37 ± 0.03b	5.70 ± 0.06a	5.31 ± 0.06b
SOC/g kg^{-1}	11.03 ± 0.52a	9.19 ± 0.96ab	7.39 ± 1.61b	8.24 ± 0.40ab
DOC/mg kg^{-1}	24.81 ± 0.74b	29.53 ± 1.93a	24.02 ± 0.43b	29.50 ± 0.30a
TN/g kg^{-1}	0.51 ± 0.04a	0.56 ± 0.02a	0.54 ± 0.02a	0.55 ± 0.03a
NO_3^--N/mg kg^{-1}	4.08 ± 0.29c	4.79 ± 0.10c	7.16 ± 0.43b	8.49 ± 0.44a
NH_4^--N/mg kg^{-1}	3.27 ± 1.23ab	1.84 ± 0.13b	2.59 ± 0.55ab	4.42 ± 0.66a
N_{min}/mg kg^{-1}	7.36 ± 1.49b	6.63 ± 0.23b	9.75 ± 0.94ab	12.92 ± 1.03a
C/N	3.59 ± 0.53ab	4.47 ± 0.36a	2.50 ± 0.22bc	2.31 ± 0.17c
MBC/mg kg^{-1}	28.37 ± 3.72c	40.29 ± 4.17ab	29.71 ± 1.91bc	44.60 ± 3.50a
BX/nmol g^{-1} h^{-1}	5.79 ± 0.65a	6.61 ± 0.06a	6.51 ± 0.40a	7.07 ± 0.41a
BG/nmol g^{-1} h^{-1}	49.03 ± 3.32c	43.52 ± 1.89c	59.45 ± 3.63b	76.30 ± 3.31a
CB/nmol g^{-1} h^{-1}	24.05 ± 0.84a	17.38 ± 0.71bc	15.66 ± 0.30c	19.11 ± 1.52b

[a]: SOC, soil total organic carbon; DOC, dissolved organic carbon; TN, total nitrogen; NO_3^--N, soil nitrate nitrogen; NH_4^--N, soil ammonium nitrogen; N_{min}, soil mineral nitrogen; C/N, soil carbon: nitrogen ratio. MBC, microbial biomass carbon. BX, BG and CB denote the activities of β-1,4-xylosidase, β-1,4-glucosidase and β-D-cellobiohydrolase, respectively. P and PO denote continuous peanut monoculture and peanut-*O. violaceus* rotation; R and B are short for the rhizosphere and bulk soil, respectively. Different lowercase letters denote the differences between treatments, at $P < 0.05$, ANOVA (± SE, $n = 3$).

3.2. Peanut rhizosphere and bulk soil microbial ecology

3.2.1 Microbial alpha diversity

A total of 1,803,157 and 1,678,154 high-quality bacterial and fungal sequences were identified from all soil samples, which were clustered into 50,088 and 46,615 OTUs, respectively. At the 97% OTU level, the overlapping and unique OTUs are illustrated by Venn diagrams (Fig. 2a and b). For bacterial OTUs, the unique OTU number was initially higher in the rhizosphere than in the bulk soil and was increased by 5.9 and 1.4 times in the rhizosphere and bulk soil, respectively. As a result, the PO rhizosphere had the highest number of bacterial unique OTUs (24.7%; 1273), with the most abundant OTUs assigned to *Pseudoxanthomonas*. For fungal OTUs, the number of unique OTUs was initially higher in the rhizosphere than in the bulk soil, and was slightly decreased by 9.3% in the rhizosphere and increased by 31.7% in the bulk soil. As a result, the P rhizosphere had the highest number of fungal unique OTUs (14.3%; 151), with the most abundant OTUs assigned to Chytridiomycota and *unclassified_f__Chaetomiaceae*. Bacterial alpha diversity indices were initially comparable in rhizosphere and bulk soil and significantly increased (by 34.4% for richness and 7.3% for diversity) in bulk soil with GM incorporation (Fig. 2c and d). The fungal alpha diversity indices were also initially comparable in the rhizosphere and in the bulk soil and significantly decreased by 23.7% with respect to richness in the rhizosphere (Fig. 2e and f).

3.2.2 Microbial community composition

For bacterial community composition, all the soil samples were dominated by Actinobacteria, Proteobacteria, Acidobacteria and Chloroflexi, which accounted for 76.8–79.7% of the total reads (Fig. 3a). At the class level, the most abundant bacterial taxa changed from Thermoleophilia in the rhizosphere of P to Alphaproteobacteria in the P bulk soil, PO rhizosphere and PO bulk soil. Compared with P, PO exhibited 85.5% and 19.9% higher relative abundances of Actinobacteria and Bacilli, respectively, and 59.2% and 29.7% lower relative abundances of Acidobacteriae and Gemmatimonadetes in the rhizosphere, respectively, while no significant difference was observed in the bulk soil. In the bulk soil, PO exhibited 55.7% higher relative abundances of *unclassified_o__Acidobacteriales*, and lower relative abundances of *Sphingomonas* and *norank_f__67 − 14* relative to P. The fungal OTUs were dominated by Ascomycota, Basidiomycota and Mortierellomycota across treatments, which occupied 90.3–97.6% of the total reads (Fig. 3b). For P, the most abundant fungal class was Sordariomycetes (38.2%) in the rhizosphere and Tremellomycetes (50.3%) in the bulk soil; for PO, the most abundant fungal classes were Tremellomycetes (29.2%) and Sordariomycetes (39.4%) in the rhizosphere and the bulk soil, respectively. Compared with P, PO exhibited 8.8 times higher relative abundances of Agaricomycetes and 51.4% lower relative abundances of Sordariomycetes in the rhizosphere, while little variation was observed in the bulk soil.

PCoA based on Bray-Curtis distances and ADONIS found a distant community structure for both bacteria and fungi (Fig. 3C and D, $P < 0.05$). For bacteria, all the treatments clustered well and separated from each other, with the distance between P and PO being farther in the bulk soil than in the rhizosphere. For fungi, the P and PO rhizosphere clustered well and separated from each other, while the P and PO bulk soil were relatively discrete and overlapped. Redundancy analysis revealed that soil pH ($R^2 = 0.70$, $P < 0.05$), SOC ($R^2 = 0.59$, $P < 0.05$) and soil water content ($R^2 = 0.47$, $P < 0.05$) were the major environmental predictors controlling bacterial community structure, collectively accounting for 59.8% of the total

community variation ($P < 0.01$, Fig. 4a). In the rhizosphere, NO_3^--N ($R^2 = 0.98$, $P < 0.01$), SOC ($R^2 = 0.96$, $P < 0.05$) and SOC/TN ($R^2 = 0.88$, $P < 0.05$) were the major environmental predictors controlling bacterial community structure, collectively accounting for 91.6% of the total community variation ($P < 0.01$, Fig. 4b). In the bulk soil, NO_3^--N ($R^2 = 0.87$, $P < 0.1$) and DOC/N_{min} ($R^2 = 0.86$, $P < 0.1$) were the major environmental predictors controlling bacterial community structure, collectively accounting for 76.7% of the total community variation ($P < 0.01$, Fig. 4c). In total, the fungal community composition was mostly controlled by DOC ($R^2 = 0.64$, $P < 0.05$) and pH ($R^2 = 0.56$, $P < 0.05$), which collectively accounted for 42.7% of the total variation ($P > 0.05$, Fig. 4d). In the rhizosphere, soil water content ($R^2 = 0.78$, $P < 0.05$) and soil pH ($R^2 = 0.55$, $P > 0.1$) were the environmental predictors controlling the bacterial community structure, accounting for 57.9% of the total community variation ($P > 0.1$, Fig. 4e). In the bulk soil, NH_4^+-N ($R^2 = 0.994$, $P < 0.01$) = pH ($R^2 = 0.993$, $P < 0.01$) > NO_3^--N ($R^2 = 0.98$, $P < 0.05$) > DOC/N_{min} ($R^2 = 0.97$, $P < 0.05$) were the main environmental predictors controlling the bacterial community structure, collectively accounting for 94.8% of the total community variation ($P < 0.1$, Fig. 4f).

3.2.3 Microbial biomarkers, co-occurrence networks and functional prediction

Groups were shown in cladograms, and LDA scores of 3.5 or greater were confirmed by LEfSe (Fig. S1 and Fig. S2). In the rhizosphere of P, 22 groups of bacteria and 16 groups of fungi were significantly enriched, namely, Acidobacteriae and Xanthobacteraceae (from phylum to genus) and *Penicillium* and Hypocreales; in the PO rhizosphere, fewer microbes were significantly enriched (19 for bacteria and 4 for fungi); and the bacteria MB-A2-108, Bacilli and the fungi *Aspergillus* and *Athelia* were enriched. In the bulk soil of P, the bacteria *Sphingomonas* and *norank_f__67 − 14* and fungi Tremellomycetes and Coniochaeta were significantly enriched; in the bulk soil of PO, the bacteria norank_p__WPS-2 and Subgroup_2 and the fungi unclassified_Ascomycota were enriched.

Taking the rhizosphere and bulk soil datasets together, microbial co-occurrence networks were constructed for P and PO based on strong and significant correlations (Fig. 5). For P, the bacterial network included 30 nodes and 58 edges; and for PO, the bacterial network included 42 nodes and 129 edges (Fig. 5A and B). Major nodes in bacterial networks belonged to Proteobacteria, Acidobacteriae and Actinobacteria for P, while those for PO belonged to Actinobacteria, Acidobacteriae and Proteobacteria. The modularity values of the bacterial networks were 0.510 and 0.442 for P and PO, respectively. The average degree, density, clustering coefficient and positive link percentage were higher for the PO bacterial network than for P, whereas the network diameter, modularity value and average path length were lower for the PO bacterial network. For P, the fungal network included 48 nodes and 286 edges; for PO, the fungal network included 45 nodes and 201 edges (Fig. 5C and D). The major nodes in the fungal networks belonged to Ascomycota and Basidiomycota for both systems. The modularity values of the fungal networks were 0.401 and 0.495 for P and PO, respectively. The network diameter, modularity values, clustering coefficient, average path length and positive link percentage were greater for PO, whereas the average degree and density were lower for the PO fungal network (Table 2).

Table 2
Topological features of co-occurrence networks constructed for soil microbial communities of P and PO treatments [a] (corresponding to Fig. 5)

Network metrics	Bacterial network		Fungal network	
	P	PO	P	PO
Average degree (AD)	3.867	6.134	11.917	8.933
Network diameter (ND)	8	7	6	9
Graph density (GD)	0.133	0.150	0.254	0.203
Modularity (MD)	0.510	0.442	0.401	0.495
Clustering coefficient (CC)	0.521	0.735	0.650	0.701
Average path length (APL)	2.841	2.619	2.034	3.087
Nodes	30	42	48	45
Edges	58	129	286	201
Positive link percentage (%)	58.6	86.8	61.7	71.6

[a] P and PO denote peanut continuous monoculture and peanut-*O. violaceus* rotation, respectively.

The composition of bacterial functional groups, inferred from the FARPROTAX database, varied between treatments (Fig. S3A). In the rhizosphere, the OTUs indicating aerobic chemoheterotrophy and chemoheterotrophy were decreased by 8.0% and 12.3% in PO than in P, while the OTUs indicating ureolysis, chitinolysis, (aromatic) hydrocarbon degradation and plastic degradation increased by 1.7 times, 22.1 times, 5.2 times, 5.2 times and 11.8 times, respectively, in PO than in P. In the bulk soil, OTUs indicating ligninolysis, aliphatic nonmethane hydrocarbon degradation and plastic degradation increased slightly and extremely by 5.8 times in PO than in P, as in the rhizosphere. In contrast, the OTUs indicating cellulolysis slightly decreased. The composition of fungal functional groups (trophic modes), inferred from the FUNGuild database, was dominated by saprotrophic fungi, pathogenic-saprotrophic-symbiotic fungi, saprotroph-symbiotic fungi and pathogenic fungi. The relative abundances of pathogenic fungi were slightly and significantly lower in PO than in P in rhizosphere and bulk soil, respectively (Fig. S3C).

3.3. Peanut rhizosphere and bulk soil K_c and its temperature sensitivity (Q_{10})

Across treatments, K_c increased with increasing temperature from 5°C to 35°C, and their correlations could be fitted with exponential growth curves (Fig. 6A and B). After averaging seven temperatures, K_c was initially significantly 26.3% higher in the bulk soil than in the rhizosphere (0.70 ± 0.03 μg CO_2 g^{-1} h^{-1}) and decreased by 23.9% ($P < 0.05$) in the bulk soil with GM incorporation, with no effect on the

rhizosphere (Fig. 6C). Conversely, Q_{10} was initially significantly higher in the rhizosphere than in the bulk soil (2.04 ± 0.08) and decreased by 13.4% ($P < 0.05$) with GM incorporation, with no effect on the bulk soil (Fig. 6D). Our results indicated significant differences in rhizosphere and bulk soil from the continuous monoculture ecosystem in terms of K_c and Q_{10}. If the rhizosphere processes were ignored, the K_c of P would be over-evaluated, and the Q_{10} of P would be underestimated. Nevertheless, such a phenomenon was not observed in PO, where there were comparable K_c (and Q_{10}) values in the rhizosphere and bulk soil. The correlation results (Tables S1 and S2) showed that K_c was positively correlated with soil C/N and negatively correlated with soil water content. Regarding the microbial taxa, K_c was positively correlated with the bacterial orders Sphingomonadales and Solirubrobacterales, and the fungal order Coniochaetales, and negatively correlated with the fungal members Glomerellales and *Chaetomium*. Q_{10} was positively correlated with the bacterial family Xanthobacteraceae and fungal phylum Ascomycota, and negatively correlated with the bacterial family Streptomycetaceae and the fungal groups Basidiomycota and Lasiosphaeriaceae. In addition, Q_{10} was negatively correlated with BG activities (Tables S3 and S4), which were positively correlated with soil water content and nitrogen contents.

3.4. Peanut bulk soil microbial ecology and C in aggregates

3.4.1 Soil processes and K_c in aggregates

For P, DOC and NH_4-N were significantly higher in the 1 − 2 mm aggregate, and TN was higher in the 0.25 − 1 mm aggregate than in the other aggregates. For PO, SOC and DOC were higher in the 1 − 2 mm aggregate, and soil pH was higher in the 0.25 − 1 mm aggregate. Compared with P, PO exhibited lower SOC in the > 2 mm and 0.25 − 1 mm aggregates and lower TN in the > 2 mm aggregate. For P, the 1 − 2 mm aggregate had the greatest K_c (1.21 ± 0.08 μg CO_2 g^{-1} h^{-1}) among aggregates, which was 21.7% higher than the corresponding fraction of PO ($P < 0.05$; Fig. 7). Q_{10} varied little among aggregates, but was lower in the PO vs. P treatment in the 0.25 − 1 mm and < 0.25 mm aggregates (11.1% and 11.4%, Table 3). For P, the contributions of different size of aggregates to SOC mineralization were 38.1%, 12.9%, 16.4% and 27.9% for the > 2 mm, 1 − 2 mm, 0.25 − 1 mm and < 0.25 mm aggregates, respectively; for PO, the contributions were 32.0%, 10.2%, 13.8% and 27.6% for the > 2 mm, 1 − 2 mm, 0.25 − 1 mm and < 0.25 mm aggregates, respectively. The contributions of the > 2 mm and < 0.25 mm aggregates were significantly higher than those of the other two aggregates for both treatments ($P < 0.05$, Fig. 7c). For the P treatment, the aggregate K_c was positively correlated with SOC and TN, and Q_{10} was positively correlated with TN, NO_3-N, NH_4-N and N_{min}. For the PO treatment, the aggregate K_c was positively corelated with SOC, while Q_{10} showed no correlation with soil properties.

Table 3
Soil biochemical properties of different size soil aggregates under P and PO treatments

Items [a]	Treatments	Aggregate sizes			
		> 2 mm	1 – 2 mm	0.25 – 1 mm	< 0.25 mm
pH	P	5.32 ± 0.03aA	5.33 ± 0.04aA	5.32 ± 0.03aA	5.28 ± 0.04aA
	PO	5.33 ± 0.02abA	5.33 ± 0.07abA	5.39 ± 0.08aA	5.22 ± 0.07bA
SOC/g kg^{-1}	P	6.46 ± 0.13aA	6.68 ± 0.09aA	6.68 ± 0.07aA	6.44 ± 0.32aA
	PO	5.62 ± 0.25cB	6.70 ± 0.39aA	6.09 ± 0.15bB	5.83 ± 0.18bcA
TN/g kg^{-1}	P	0.69 ± 0.02abA	0.72 ± 0.05aA	0.63 ± 0.02bA	0.68 ± 0.02abA
	PO	0.58 ± 0.01aB	0.59 ± 0.03aA	0.59 ± 0.06aA	0.62 ± 0.04aA
DOC/mg kg^{-1}	P	85.04 ± 11.23cA	97.14 ± 11.07aA	90.73 ± 10.61bA	87.79 ± 11.48bcA
	PO	70.88 ± 11.87bA	75.36 ± 10.02aA	71.38 ± 10.89bA	70.65 ± 10.11bA
NO_3^--N/mg kg^{-1}	P	46.59 ± 5.41aA	48.49 ± 5.79aA	48.44 ± 5.30aA	47.74 ± 5.62aA
	PO	47.56 ± 1.45aA	48.93 ± 2.82aA	47.50 ± 2.53aA	49.69 ± 3.25aA
NH_4^--N/mg kg^{-1}	P	14.73 ± 2.81bA	17.13 ± 3.45aA	15.94 ± 2.86abA	16.90 ± 2.74aA
	PO	13.88 ± 2.12aA	13.29 ± 1.85aA	13.60 ± 2.69aA	11.77 ± 0.62aA
N_{min}/mg kg^{-1}	P	61.31 ± 8.22aA	65.62 ± 9.24aA	64.38 ± 7.91aA	64.63 ± 8.24aA
	PO	61.43 ± 2.42aA	62.22 ± 3.25aA	61.10 ± 4.27aA	61.47 ± 3.24aA
C/N	P	1.47 ± 0.32aA	1.57 ± 0.32aA	1.47 ± 0.28aA	1.43 ± 0.30aA
	PO	1.15 ± 0.16aA	1.21 ± 0.12aA	1.16 ± 0.12aA	1.15 ± 0.14aA
MBC/mg kg^{-1}	P	37.62 ± 16.18aA	34.77 ± 12.71aA	34.84 ± 9.88aA	35.47 ± 17.04aA
	PO	24.46 ± 7.40aA	19.95 ± 4.18aA	25.22 ± 7.15aA	28.74 ± 4.37aA
Soil enzyme activities					

Items [a]	Treatments	Aggregate sizes			
		> 2 mm	1 – 2 mm	0.25 – 1 mm	< 0.25 mm
BX/nmol g^{-1} h^{-1}	P	3.43 ± 0.16aA	2.85 ± 0.37aA	3.40 ± 0.24aA	3.10 ± 0.61aA
	PO	3.31 ± 0.32aA	2.82 ± 0.20aA	2.70 ± 0.29aA	3.19 ± 0.02aA
BG/nmol g^{-1} h^{-1}	P	23.09 ± 6.44aA	24.97 ± 3.00A	42.78 ± 25.06A	20.71 ± 0.58A
	PO	18.80 ± 0.27bA	17.51 ± 1.49bA	20.51 ± 2.60abA	24.03 ± 1.66aA
CB/nmol g^{-1} h^{-1}	P	21.15 ± 2.05aA	16.50 ± 6.15aA	14.32 ± 2.69aA	15.73 ± 1.60aA
	PO	15.45 ± 3.58aA	14.04 ± 2.97aA	17.76 ± 6.26aA	14.14 ± 2.95aA
K_c/μg CO_2 g^{-1} h^{-1}	P	0.93 ± 0.07bA	1.21 ± 0.08aA	0.94 ± 0.06bA	0.90 ± 0.09bA
	PO	0.84 ± 0.04aA	0.95 ± 0.09aB	0.84 ± 0.05aA	0.79 ± 0.04aA
Q_{10}	P	1.83 ± 0.07aA	2.01 ± 0.09aA	1.95 ± 0.05aA	1.85 ± 0.03aA
	PO	1.86 ± 0.12aA	1.85 ± 0.08aA	1.73 ± 0.03aB	1.64 ± 0.03aB

[a] SOC, soil total organic carbon; DOC, dissolved organic carbon; TN, total nitrogen; NO_3^--N, soil nitrate nitrogen; NH_4^--N, soil ammonium nitrogen; N_{min}, soil mineral nitrogen; C/N, soil carbon: nitrogen ratio. MBC, microbial biomass carbon. BX, BG, and CB denote the activities of β-1,4-xylosidase, β-1,4-glucosidase, and β-D-cellobiohydrolase. P and PO denote continuous peanut monoculture and peanut-*O. violaceus* rotation, respectively. Different lowercase letters denote the differences among aggregates, while different capital letters indicate the differences between treatments at $P < 0.05$, ANOVA (± SE, $n = 3$).

3.4.2 Bacterial communities in aggregates

Approximately 90,614 and 94,801 high-quality sequence reads for bacteria were generated for the P and PO samples, respectively, across aggregates. The numbers of reads from the P and PO treatments were on average 2521 ± 77 and 2661 ± 59 per sample for bacteria, respectively. There were no significant differences between the different sizes of aggregates in the overall microbial diversity, as measured by the number of OTUs and Chao1, ACE, Shannon and Simpson diversity indices (Table S5). However, the number of OTUs and Chao1 and ACE diversity indices were significantly higher in the PO vs. P treatment only in the > 2 mm aggregate, which suggested that the > 2 mm aggregate may be more sensitive to GM inclusion and that bacterial communities from the PO treatment were richer. qPCR analysis showed that there were no differences between the total number of bacteria between treatments, regardless of the size of the soil aggregates (Fig. S4), with concentrations numerically higher in the P vs. PO treatments. Taxon-specific qPCR analysis showed that the relative abundance of Patescibacteria (class

Saccharimonadia) and Verrucomicrobia (class Verrucomicrobiae) was highest in the < 0.25 mm aggregate, compared with the other three aggregates. In addition, the 1 − 2 mm aggregate exibited the highest relative abundance of Rhizobiales (genus *Allorhizobium-Neorhizobium-Pararhizobium-Rhizobium*) in the P treatment and the most abundant Xanthomonadales (genus *Dyella*) in both treatments. Moreover, T test analysis showed that the > 2 mm and < 0.25 mm aggregates were more responsive than the other two aggregates (Table S6). Correlation analysis (Table S7) showed that Q_{10} was positively correlated with the relative abundance of the orders Betaproteobacteriales, Bacillales and Xanthomonadales, while K_c was positively correlated with only that of the genera *Allorhizobium-Neorhizobium-Pararhizobium-Rhizobium* and *Dyella*.

3.4.3 Carbon degradation genes

In this study, metabolic genes involved in the degradation of starch, pectin, hemicellulose, cellulose, chitin, and lignin were detected in all samples (Fig. 8). No difference across aggregates or between treatments was observed with the bulk soil genes (Fig. S5). qPCR analysis detected 14, 15, 15, 15 and 13, 14, 13, 14 carbon degradation genes in the P and PO treatments for the > 2 mm, 1 − 2 mm, 0.25 − 1 mm and < 0.25 mm aggregates, respectively. Specifically, the abundance (measured as concentration) of genes involved in the degradation of moderately labile C, such as cex involved in cellulose degradation, was significantly lower in the PO vs. P treatment in the 0.25 − 1 mm and < 0.25 mm aggregates. The abundance of genes involved in the degradation of recalcitrant C, such as chiA, involved in chitin-degrading genes was lower in the PO treatment in the 1 − 2 mm and < 0.25 mm aggregates, and the abundances of mnp, involved in lignin-degrading genes, was lower in the 0.25 − 1 mm aggregates. Overall, soil aggregates (except > 2 mm aggregate) from the PO treatment had a significantly lower abundance for the genes encoding enzymes for moderately labile C and recalcitrant C. In contrast, the functional genes involved in C fixation, such as aclB and acsB were promoted in the > 2 mm and 1 − 2 mm aggregates by 90.6% and 54.5%, respectively. Correlation analysis showed that BG activities were correlated with the concentrations of functional genes such as abfA involved in hemi-cellulose degradation and glx involved in lignin degradation, while CB activities were correlated with the concentrations of functional genes such as pgu involved in pectin degradation and abfA and manB involved in hemi-cellulose degradation ($P < 0.05$; Table S8). Moreover, K_c was positively correlated with the concentrations of abfA and xylA, and Q_{10} was positively correlated with that of xylA. In addition, the relative abundance of Gammaproteobacteria (family Enterobacteriaceae) positively correlated with the functional genes involved in pectin (pgu), hemi-cellulose (abfA, manB, xylA), cellulose (cdh, cex), chitin (chiA) and lignin (mnp). Significant correlations of this subgroup with all the genes involved in C degradation indicated their importance in C degradation gene production and their pivotal role in C mineralization.

4. Discussion

4.1. GM improved soil water, pH and especially N contents

Initially, for the P treatment, the rhizosphere was characterized by a less preferable niche for soil microorganisms relative to the bulk soil, with significantly lower labile C (i.e., DOC and MBC, Table 1). Despite the slightly higher SOC due to the continuous inputs of root exudates and rhizodeposition, lower labile C suggested higher recalcitrant C in rhizosphere vs. bulk soil, which may be related to the altered chemical composition of root exudation associated with continuous monoculture obstacles (Bao et al. 2022). Typical autotoxic substances such as phenolic acids have been reported to be released through plant root exudation in continuous cropping (Wang et al. 2023), which probably drive the rhizosphere SOC pool toward being more recalcitrant (Olk et al. 2000). In contrast, the significantly higher DOC and MBC in bulk soil vs. rhizosphere both with and without GM inclusion were likely derived from the root residues and exudation of peanuts, which accumulated yearly under continuous monoculture. As a result, the rhizosphere was characterized by less abundant Alphaproteobacteria and Actinobacteria than the bulk soil (Fig. 3a), documented as copiotrophic, and more abundant Acidobacteriae relative to the bulk soil, known as oligotrophic (Fierer et al. 2007).

After seven years *O. violaceus* incorporation as GM, 1) the roots of GM could effectively dredge the soil, increase the soil porosity, and promote the capacity of soil water and fertilizer retention; and 2) after the GM was turned over and returned to the field, it could increase the water-stable aggregates and the ability to store water and retain moisture, thus resulting in improvements in soil water in both rhizosphere and bulk soil (Table 1). *O. violaceus* itself has a high protein content (Zhao et al. 2010), which is beneficial for subsequent crops because of the nutrients (especially N) that are released when their residues are returned to soils (Xu et al. 2023). Specially, in the rhizosphere, the enhanced nitrogen fixation by nodules led to an increase in NO_3^--N by 75.5%, while the altered root exudates and rhizosphere metabolites led to an increase in pH by 0.3 units (Table 1). Legumes release protons during the process of biological nitrogen fixation; thus, *O. violaceus* inclusion could be effective at increasing soil pH mostly by changing root exudates and rhizosphere metabolites, causing soil nutrients to be more conducive to crop absorption. In the bulk soil, the additional N resourced by GM caused an equivalent increase in NO_3^--N (by 77.3%) to the rhizosphere and additionally enhanced NH_4^+-N by 140.3%, leading to further reduced DOC/N_{min} (Table 1). A previous study reported that residues with only a C/N ratio below 24 induced a surplus of N_{min} (Trinsoutrot et al. 2000), and soils with a low C/N ratio may be characterized by slower N immobilization and a surplus of available N, favoring residue decomposition and mineralization (Zhou et al. 2020).

4.2 GM optimized microbial communities, including the promotion of plant growth-promoting microbes and pathogen inhibition

In this study, *O. violaceus* was beneficial for subsequent peanut growth by improving microbial communities mainly as a nitrogen resource. *O. violaceus* incorporation drove the divergent responses of bacterial alpha diversity in rhizosphere (unchanged) and bulk soil (increased), especially through NH_4^+-N, as NO_3^--N and NH_4^+-N are exclusive N resources for bacteria in agricultural ecosystems and participate

in protein synthesis in bacteria (Bottomley et al. 2012), which was confirmed by their positive correlation (Table S1). In contrast, the reduction in fungal richness in the rhizosphere might be caused by the higher soil pH, confirmed by their negative correlation (Table S2). Soil pH is one of the most important environmental factors that affects soil fungi, and fungi prefer to grow in more acidic environments (Liu et al. 2018a). Alternatively, GM-induced changes in root exudation and metabolites can reduce rhizosphere fungal richness, probably by recruiting specific fungal species (Wu et al. 2021). Divergent responses of bacterial and fungal alpha diversity clearly indicated their distinct metabolic separation and resource preferences. A shift in microbial community composition could be reflected by microbial substrate utilization, i.e., enzyme patterns. The higher BG activities in PO, especially in the bulk soil (Table 1), suggested enhanced decomposition of recalcitrant C due to incorporation of the *O. violaceus* residues. Accordingly, the bacterial family Streptomycetaceae and fungal order Glomerellales, which were positively correlated with BG activities (Table S3 and S4), were enhanced in both rhizosphere and bulk soil in PO due to their capacity to degrade highly recalcitrant organic materials (Barka et al. 2016). In contrast, lower CB activities in the PO rhizosphere were likely related to a decrease in root-derived C, i.e., root biomass (Fig. 1b). Accordingly, bacterial taxa (Acidobacteriota and Chloroflexi) and fungal genera (*Penicillium, Fusarium, Trichoderma* and *Thielavia*) that positively correlated with CB activities (Tables S3 and S4) were suppressed in the rhizosphere. The enzyme patterns corresponded well with the functional annotation, which predicted promoted decomposition of recalcitrant C but inhibited cellulolysis (Fig. S3a).

Green manuring can reshape the composition of soil and root-associated microbes (Zhang et al. 2017). First, incorporation of GM introduced a large amount of debris with C and N substrates into soil and directly stimulated important lignocellulose decomposers such as Agaricomycetes (Sinsabaugh et al. 2005) by 8.8 times in the rhizosphere, and *Chaetomium* (Banerjee et al. 2016) by 95.0% and Acidobacteriae (Kalam et al. 2020) by 34.4% in bulk soil (Fig. 3). Moreover, GM incorporation provided more suitable habitat for microorganisms (higher soil pH, water content) by improving root exudation and metabolites, thereby supporting more beneficial microbes, such as the phosphorus-solubilizing fungus *Aspergillus* (by 30.0 times) (KOUR et al. 2021) and the plant growth-promoting fungus *Naganishia* (by 3.2 times) (Tapia-Vázquez et al. 2020), and less acidophilic and oligotrophic Acidobacteriae (Kalam et al. 2020) in the PO rhizosphere. One of the bacteria enriched in the rhizosphere of PO was Bacillus (Fig. S1), well known as phosphorus-solubilizing bacteria and plant growth-promoting bacteria (KOUR et al. 2021; Xie et al. 2009). In a previous study at the same site, Bacilli was verified to be regulated by available phosphorus and positively correlated with enhanced peanut yields (Wu et al. 2023b). The relevant mechanism may be as follows: Inclusion of *O. violaceus* as a GM probably activated insoluble phosphorus in the soil to become available phosphorus through the large amount of organic acids secreted by the root systems and many soluble organic compounds generated after being buried and decayed (Zhao et al. 2010) and further recruited phosphorus-solubilizing microorganisms in the crop rhizosphere (Zhang et al. 2022). Moreover, during the decay course of GM after planting and flipping, large amounts of secondary metabolites, enzymes and volatile compounds are produced and released, which can directly promote crop growth and enhance crop resistance to disease. The inhibition

of pathogenic fungi, such as *Fusarium* by 49.6% in the rhizosphere (Fig. 3b), was predicted by functional annotation (Fig. S3). In addition, we found slight enrichment of *Gaiella* (Actinobacteria) in the PO rhizosphere, which is one of several identified bioindicators of high biological soil health ratings (Wilhelm et al. 2023). Therefore, GM crops aid in the optimization of soil microbial community composition for plant growth-promoting microbe enhancement and pathogen inhibition (Ding et al. 2021), thereby alleviating continuous cropping obstacles and enhancing yields.

4.3 GM decreased the bulk soil K_c and the rhizosphere Q_{10} via strengthened C limitation

For P, K_c was initially higher in the bulk soil than in the rhizosphere due to the greater DOC and MBC in the bulk soil (Table 1), as K_c was mainly related to the labile C pool. The bulk soil provided a more favorable environment for microbial activities through increased nutrients, leading to significant increases in microbial biomass, thus promoting soil C mineralization. After the GM was returned to the field, a series of physicochemical and biological reactions took place in the microzone of its residues during the process of decomposition, which affected the soil C dynamics. In the rhizosphere, the unchanged K_c could be attributed to the unchanged DOC and MBC (Table 1) due to the constant flux of root exudation. In the bulk soil, the reduced K_c (by 23.9%, Fig. 6) could be attributed to multiple mechanisms. One possibility (I) is that microbes from the peanut fields may suffer from C limitation, considering the initially lower SOC/TN than the most appropriate ratio (< 25:1), which was confirmed by the positive correlation between K_c and soil DOC/N_{min} (Table S1). It is crucial to determine whether soil microbes are limited by energy (Fontaine et al. 2004). If soil microbes are not limited, then SOC accumulation should be related to the fresh organic matter input; in contrast, if soil microbes are limited then greater fresh organic matter input could result in higher SOC turnover. The impact of fresh organic residue input on SOC mineralization, therefore, may be interpreted in light of microbial competition. The further reduced soil DOC/N_{min} ratio with GM incorporation (Table 1) may exacerbate the competition of C sources, leading to a negative priming effect (Chen et al. 2019). With GM incorporation, the strengthened C limitation probably stimulated *K*-strategist SOC decomposers (e.g., Acidobacteria, Glomerellales and *Chaetomium*), as evidenced by the enhanced BG activities (Table 1), and constrained the *r*-strategist SOC decomposer (e.g., Sphingomonas, norank_f__67 − 14 and *Coniochaeta*) in the bulk soil, as indicated by the lower K_c. This pattern agreed with a previous study providing evidence that microbial competition is an important determinant of SOC mineralization (Fontaine et al. 2004). Moreover, from microbial network relationships (Fig. 5), GM incorporation shifted the predominant taxa from the copiotrophic Proteobacteria to the saprotrophic and oligotrophic Actinobacteria (Barka et al. 2016) in the bacterial network and from Ascomycota preferring to use the easily degradable fractions of residues (Liu et al. 2018a) to Ascomycota together with Basidiomycota specializing in utilizing complex lignocellulose components (Sinsabaugh et al. 2005) in the fungal network. Therefore, the lower bulk soil K_c was probably a result of the microbial niche changing to be more recalcitrant and the dominance of *K*-strategist SOC decomposers under strengthened C limitation. Another possibility (□) is that GM incorporation may have promoted the SOC mineralization rate, i.e., the fresh organic matter input

induced a real priming effect, which should be verified in the future. Furthermore, at the beginning of returning, the fresh body of *O. violaceus* decays fast, as it contains a large amount of labile organic matter that can provide carbon resources and nutrients for microorganisms; with the extension of flipping time, the easily decomposable organic matter in the GM residues gradually decreases, while the proportion of recalcitrant crude fibers, lignin, etc., increases, thus resulting in a relatively slower mineralization rate at our sampling. This was confirmed by the C/N ratio of *O. violaceus* increasing from the initial 9.7 to 15.3 after 126 days' of decomposition (Liu et al. 2013). In this case, our results represented only a single time point and variations in phenological differences cannot be considered, which is the drawback of this study. Nevertheless, previous studies have shown that long-term patterns within soil microbial communities generally remain intact and reflect differences in management practices (Trivedi et al. 2015).

The initially higher rhizosphere Q_{10} in P was likely related to the lower substrate quality than in the bulk soil (Table 1). With GM inclusion, the neutral response of the bulk soil Q_{10} likely resulted from the unchanged labile substrate availability (DOC and MBC). However, the reduced rhizosphere Q_{10} (by 13.4%, Fig. 6) was directly related to the decreased SOC, as the rhizosphere Q_{10} was more likely controlled by substrate availability than quality (Bosatta and Ågren 1999). From the perspective of microbial communities, Q_{10} was positively correlated with Ascomycota and negatively correlated with Basidiomycota since Ascomycota prefer to use the easily degradable fractions of residues, and Basidiomycota can degrade complex lignocellulose components (Liu et al. 2018a). Similarly, positive correlations between Q_{10} and Xanthobacteraceae were ascribable to their susceptibility to labile C, confirmed by their positive correlation with CB activities, while negative correlations of Q_{10} with Streptomycetaceae were related to their relevance in BG activities. Therefore, the lower rhizosphere Q_{10} could also be related to the decreased percentage of Xanthobacteraceae and Ascomycota and to the increased percentage of Streptomycetaceae and Basidiomycota (Fig. 3). Overall, GM inclusion decreased the bulk soil K_c and the rhizosphere Q_{10}, which generally supported our first hypothesis. Therefore, the initially different soil conditions in the rhizosphere and bulk soil resulted in divergent responses of microbial communities and their regulated C dynamics, supporting the second hypothesis.

Unexpectedly, P vs. PO had a higher SOC sequestration relative to the initial level (26.7% vs. 19.5%) via rhizosphere SOC sequestration and N fixation processes (Virk et al. 2022). This indicated that the continuous peanut monoculture system had relatively greater SOC sequestration potential without stubble incorporation. The rhizosphere-derived recalcitrant compounds of legumes accumulated in soil over the years and therefore could enhance the long-term storage of SOC, which should be verified in the future. Many studies have demonstrated that agricultural activities involving GM are crucial in SOC sequestration (GAO et al. 2023; Muhammad et al. 2022). However, carbon input to soil may not necessarily increase the soil carbon content (Fontaine et al. 2004). Indeed, *O. violaceus* incorporation showed no advantage in the bulk SOC accumulation (Table 1), despite the positive effect on soil and microbial properties. This could be interpreted as the effect of GM induced C supply being counteracted by that of the affected SOC mineralization to CO_2, which reinforced the microbial C limitation (Fontaine et

al. 2004). Such a pattern has been reported previously, which was ascribable to the priming effect (Liu et al. 2014). In Liu et al.'s experiment, SOC in the *O. violaceus* applied treatment showed no difference from the control after the first 15 days. A previous report (Elfstrand et al. 2007) also suggested that the effect of GM-based rotation on C accumulation may be limited. The low C/N ratio of the GM crop may be a major explanatory factor in this unexpected nonsignificant response of SOC, which strengthened the C limitation. Nevertheless, increases in soil bacterial diversity, communities and interactions and inhibition of K_c and Q_{10} resulting from GM-based rotation may benefit soil health and mitigate the genitive effects of climate change. Moreover, the rhizosphere reduced SOC, and the unchanged SOC mineralization led us to conclude that the reduction in SOC accumulation was possibly due to a reduction in underground C allocation, which is inversely proportional to N availability. On the other hand, the reduced rhizosphere SOC suggested enhancement of absorption and consumption of rhizosphere C sources by plants and microorganisms. Crop rotation can promote the full utilization of nutrient resources of the main crop. The root exudates of GM crops affected peanut growth, and their complementary ecological niches widened the space for peanuts to use nutrients, thereby affecting the absorption and utilization of rhizosphere C sources. Ultimately, PO exhibited comparable K_c, Q_{10} and SOC levels in rhizosphere and bulk soil (Fig. 6), suggesting that the 'rhizosphere effect' was cancelled and the dispersal of C mineralization across compartments was facilitated.

4.4. Soil aggregates mediated the GM effect on functional genes

Minor variation has been observed with the microbial communities across aggregates or between treatments (bulk soil) at the same class of aggregate (Table S5, Table S7; Fig. 8), as the difference between legumes and nonlegumes was usually significant, while those between the legume-based rotations tended to be small (Trivedi et al. 2015). Nevertheless, we can obtain a glimpse of different C mineralization, C fractions, SOC-degradation enzyme activities and functional genes involved in C cycling through investigation at the aggregate level. For P treatment, the 1 − 2 mm aggregate harbored higher DOC and N levels (Table 3) and supported the most abundant Rhizobiales (genus *Allorhizobium-Neorhizobium-Pararhizobium-Rhizobium*) and Xanthomonadales (genus *Dyella*) (Table S6), which were assigned to the copiotroph (*r*-strategists) using labile forms of C for growth and metabolism, and grew faster in a nutrient rich environment (Fierer et al. 2007), thus determining the higher K_c compared with other aggregates. This was consistent with a previous study reporting that the 1 − 2 mm aggregate was a hotpot in a fragmented soil environment with a higher SOC mineralization rate (Rui et al. 2022). Nevertheless, such a pattern was not observed in the PO treatment, where there was comparable K_c and Q_{10} across aggregates despite the higher SOC and DOC in the 1 − 2 mm aggregate. We speculated that GM incorporation homogenized the C mineralization across aggregates by facilitating dispersal (Liang et al. 2023), via the homogeneously incorporated residues and/or the physical disturbance associated with GM incorporation, such as tillage (West et al. 2023). The reduced Q_{10} in the 0.25 − 1 mm and < 0.25 mm aggregates (Table 3) suggested that the temperature response of the stored C may be limited under PO

treatments, as the deposition and retention of C in microaggregates is more likely to explain the stored C.

Although the 1 − 2 mm aggregate had the highest K_c, the > 2 mm and < 0.25 mm aggregates contributed the most of the K_c, SOC and DOC for both treatments (Fig. 7c). The > 2 mm and 0.25 − 1 mm aggregates of PO exhibited a lower contribution to SOC than P, while the other two aggregates showed no significant difference between treatments, leading to a 10.1% lower ($P > 0.05$) contribution ratio of SOC in the PO vs. P treatment. In addition, positive correlations between K_c and SOC, as well as between Q_{10} and N fractions, highlighted the regulatory role of substrate quality in soil C mineralization dynamics at the aggregate scale (Li et al. 2023). However, such a pattern was not observed with MBC in the PO treatment, which showed no significant difference between aggregates, in contrast to the P treatment which exhibited a higher contribution ratio in the > 2 mm and < 0.25 mm aggregates. This probably suggested that the effect of the facilitated dispersal extends to microbial biomass production, which agrees with the comparable K_c and Q_{10} between aggregates. Notably, the PO treatment suppressed genes encoding enzymes for moderately labile C and recalcitrant C degradation (Fig. 8), likely because the microbial communities prefer labile C to recalcitrant C, especially under high-quality substrate addition (Fierer et al. 2007), leading to reduced degradation of relatively more recalcitrant C. This, together with the promotion of genes encoding enzymes for C fixation, indicated that soil C storage may be improved and the temperature response may be limited under GM incorporation in the future. Moreover, positive correlations between K_c and the relative abundances of abfA and xylA (Table S7) suggested the relevance of hemicellulose mineralization to CO_2 emissions, and positive correlations between Q_{10} and the relative abundances of xylA suggested that the specific carbon substrate is more responsive to temperature changes.

5. Conclusion

In the continuous peanut monoculture ecosystem, incorporation of *O. violaceus* as a GM for seven years not only increased yields but also reduced the rhizosphere Q_{10} and the bulk soil SOC mineralization, and alleviated the continuously monocultured obstacle through optimizing microbial communities, thus being a cleaner and recommendable production practice, thereby contributing to carbon neutralization. Our results provided direct evidence that GM (Cruciferae, C/N < 25) reduces the soil carbon mineralization of the legume' field from the perspectives of compartments and aggregates. The rhizosphere Q_{10} was reduced due to increased consumption and therefore, reduced SOC. In the bulk soil, the N surplus and the further reduced C/N indicated intensified soil C limitation, which leads to the negative priming effect. From the microbial network relationships, the predominant taxa shifts from copiotrophic Proteobacteria to saprotrophic and oligotrophic Actinobacteria. At the aggregate scale, inhibition of genes involved in C mineralization and promotion of genes involved in C fixation can positively affect soil C storage in the future. The microbial variations contribute to the suppressed K_c in the bulk soil. Ultimately, PO exhibits comparable K_c, Q_{10} and SOC levels in rhizosphere and bulk soil, and comparable MBC, K_c and Q_{10} across aggregates, suggesting that GM incorporation might homogenize

SOC mineralization across compartments by facilitating dispersal. These results highlighted the regulatory mechanism of both compartments and aggregates on microbial diversity, community composition and their involved C mineralization, which should be properly accounted for when simulating the GM effects on a regional agroecosystem carbon balance.

Abbreviations

GM: green manure

P: continuous peanut monoculture

PO: peanut-*Orychophragmus violaceus* rotation

R: rhizosphere soil

B: bulk soil

SOC: soil organic carbon

K_c: SOC mineralization rate

Q_{10}: temperature sensitivity of SOC mineralization

C/N1: soil dissolved carbon: mineral nitrogen ratio

C/N2: soil total organic carbon content: total nitrogen ratio

NO_3^--N: soil nitrate nitrogen

NH_4^+-N: soil ammonium nitrogen

DOC: soil dissolved organic carbon

MBC: microbial biomass carbon

TN: soil total nitrogen

BX: β-1,4-xylosidase activity

BG: β-1,4-glucosidase activity

CB: β-D-cellobiohydrolase activity

Declarations

Acknowledgements

This work is supported by the Natural Science Foundation of China (No. 32301451), Natural Science Foundation of Shandong Province (ZR202103030197, ZR2020QC121), Central Guidance for Local Scientific and Technological Development Project (YDZX2022131) and Taishan Scholars Program.

Author contributions

Q.Q. Sun designed this study and wrote the first draft of the manuscript; Y.M. Zheng performed the experiment; X.W. Sun and L.J. Wu analyzed the data; Z.F. Wu and J.L. Zhang wrote the paper; T.Y. Yu, S. B. Wan and J.C. Zhang acquired the fund and revised the paper. All authors read and approved the final manuscript.

Conflict of interest The authors declare no competing interests.

References

1. Banerjee S, Kirkby CA, Schmutter D, Bissett A, Kirkegaard JA, Richardson AE (2016) Network analysis reveals functional redundancy and keystone taxa amongst bacterial and fungal communities during organic matter decomposition in an arable soil. Soil Biology and Biochemistry 97: 188-198. doi: https://doi.org/10.1016/j.soilbio.2016.03.017.
2. Bao L, Liu Y, Ding Y, Shang J, Wei Y, Tan Y, Zi F (2022) Interactions Between Phenolic Acids and Microorganisms in Rhizospheric Soil From Continuous Cropping of Panax notoginseng. Frontiers in Microbiology 13: 791603. doi: http://dx.doi.org/10.3389/fmicb.2022.791603.
3. Barka EA, Vatsa P, Sanchez L, Gaveau-Vaillant N, Jacquard C, Klenk HP (2016) Taxonomy, Physiology, and Natural Products of Actinobacteria. Microbiology Molecular Biology Reviews 8: 1-43. doi: http://dx.doi.org/10.1128/MMBR.00044-16.
4. Bian Q, Wang X, Bao X, Zhu L, Xie Z, Che Z, Sun B (2022) Exogenous substrate quality determines the dominant keystone taxa linked to carbon mineralization: Evidence from a 30-year experiment. Soil Biology and Biochemistry 169: 108683. doi: https://doi.org/10.1016/j.soilbio.2022.108683.
5. Bosatta E, Ågren GI (1999) Soil organic matter quality interpreted thermodynamically. Soil Biology and Biochemistry 31: 1889-1891. doi: https://doi.org/10.1016/S0038-0717(99)00105-4.
6. Bottomley P, Taylor A, Myrold D (2012) A consideration of the relative contributions of different microbial subpopulations to the soil N cycle. Frontiers in microbiology 3: 373. doi: http://dx.doi.org/10.3389/fmicb.2012.00373.
7. Caporaso JG, Lauber CL, Walters WA, Berg-Lyons D, Lozupone CA, Turnbaugh PJ, Fierer N, Knight R (2011) Global patterns of 16S rRNA diversity at a depth of millions of sequences per sample. Proceedings of the National Academy of Sciences of the United States of America 108 Suppl 1: 4516-4522. doi: https://doi.org/10.1073/pnas.1000080107.
8. Casamayor E (2012) Using network analysis to explore co-occurrence patterns in soil microbial communities. ISME J 6: 343-351. doi: http://dx.doi.org/10.1038/ismej.2011.119.

9. Chen L, Jiang Y, Liang C, Luo Y, Xu Q, Han C, Zhao Q, Sun B (2019) Competitive interaction with keystone taxa induced negative priming under biochar amendments. Microbiome 7: 77. doi: http://dx.doi.org/10.1186/s40168-019-0693-7.
10. Dai Z, Zang H, Chen J, Fu Y, Wang X, Liu H, Shen C, Wang J, Kuzyakov Y, Becker JN, Hemp A, Barberán A, Gunina A, Chen H, Luo Y, Xu J (2021) Metagenomic insights into soil microbial communities involved in carbon cycling along an elevation climosequences. Environmental Microbiology 23: 4631-4645. doi: https://doi.org/10.1111/1462-2920.15655.
11. Davidson EA, Belk E, Boone RD (1998) Soil water content and temperature as independent or confounded factors controlling soil respiration in a temperate mixed hardwood forest. Global Change Biology 4: 217-227. doi: https://doi.org/10.1046/j.1365-2486.1998.00128.x.
12. Davinic M, Fultz LM, Acosta-Martinez V, Calderón FJ, Cox SB, Dowd SE, Allen VG, Zak JC, Moore-Kucera J (2012) Pyrosequencing and mid-infrared spectroscopy reveal distinct aggregate stratification of soil bacterial communities and organic matter composition. Soil Biology and Biochemistry 46: 63-72. doi: https://doi.org/10.1016/j.soilbio.2011.11.012.
13. Ding F, Sun W, Huang Y, Hu X (2017) Larger Q_{10} of carbon decomposition in finer soil particles does not bring long-lasting dependence of Q_{10} on soil texture. European Journal of Soil Science 69: 336-347. doi: https://doi.org/10.1111/ejss.12530.
14. Ding T, Yan Z, Zhang W, Duan T (2021) Green Manure Crops Affected Soil Chemical Properties and Fungal Diversity and Community of Apple Orchard in the Loess Plateau of China. Journal of Soil Science and Plant Nutrition 21: 1089-1102. doi: http://dx.doi.org/10.1007/s42729-021-00424-0.
15. Du L, Wang R, Hu Y, Li X, Gao S, Wu X, Gao X, Yao L, Guo S (2021) Contrasting responses of soil C-acquiring enzyme activities to soil erosion and deposition. CATENA 198: 105047. doi: https://doi.org/10.1016/j.catena.2020.105047.
16. Edgar RC (2013) UPARSE: highly accurate OTU sequences from microbial amplicon reads. Nature Methods 10: 996-998. doi: https://doi.org/10.1038/nmeth.2604.
17. Elfstrand S, Hedlund K, Mårtensson A (2007) Soil enzyme activities, microbial community composition and function after 47 years of continuous green manuring. Applied Soil Ecology 35: 610-621. doi: https://doi.org/10.1016/j.apsoil.2006.09.011.
18. Fierer N, Bradford MA, Jackson RB (2007) Toward an ecological classification of soil bacteria. Ecology 88: 1354-1364. doi: https://doi.org/10.1890/05-1839.
19. Fontaine S, Bardoux G, Abbadie L, Mariotti A (2004) Carbon input to soil may decrease soil carbon content. Ecology Letters 7: 314-320. doi: https://doi.org/10.1111/j.1461-0248.2004.00579.x.
20. Forte A, Fagnano M, Fierro A (2017) Potential role of compost and green manure amendment to mitigate soil GHGs emissions in Mediterranean drip irrigated maize production systems. Journal of Environmental Management 192: 68-78. doi: http://dx.doi.org/10.1016/j.jenvman.2017.01.037.
21. GAO S-j, LI S, ZHOU G-p, Cao W-d (2023) The potential of green manure to increase soil carbon sequestration and reduce the yield-scaled carbon footprint of rice production in southern China. Journal of Integrative Agriculture 22: 2233-2247. doi: http://dx.doi.org/10.1016/j.jia.2022.12.005.

22. He S, Chen Y, Xiang W, Chen X, Wang X, Chen Y (2021) Carbon and nitrogen footprints accounting of peanut and peanut oil production in China. Journal of Cleaner Production 291: 125964. doi: https://doi.org/10.1016/j.jclepro.2021.125964.
23. Ho LH, Un KS, Ri HH, Yeong HD, N. OV, Sandeep K, Oh HC (2021) Mitigation of global warming potential and greenhouse gas intensity in arable soil with green manure as source of nitrogen J Environmental Pollution 288: 117724. doi: https://doi.org/10.1016/j.envpol.2021.117724.
24. Hwang HY, Cuello J, Kim SY, Lee JG, Kim PJ (2020) Green manure application accelerates soil organic carbon stock loss under plastic film mulching. Nutrient Cycling in Agroecosystems 116: 257-269. doi: http://dx.doi.org/10.1007/s10705-019-10042-z.
25. Kalam S, Basu A, Ahmad I, Sayyed R, El Enshasy H, Joe Dailin D, Suriani N (2020) Recent Understanding of Soil Acidobacteria and Their Ecological Significance: A Critical Review. Frontiers in Microbiology 11: 580024. doi: http://dx.doi.org/10.3389/fmicb.2020.580024.
26. KOUR D, RANA KL, KAUR T, YADAV N, YADAV AN, KUMAR M, KUMAR V, DHALIWAL HS, SAXENA AK (2021) Biodiversity, current developments and potential biotechnological applications of phosphorus-solubilizing and-mobilizing microbes: A review. Pedosphere 31: 43-75. doi: http://dx.doi.org/10.1016/S1002-0160(20)60057-1.
27. Kuzyakov Y, Friedel JK, Stahr K (2000) Review of mechanisms and quantification of priming effects. Soil Biology and Biochemistry 32: 1485-1498. doi: https://doi.org/10.1016/S0038-0717(00)00084-5.
28. Lefèvre R, Barré P, Moyano FE, Christensen BT, Bardoux G, Eglin T, Girardin C, Houot S, Ktterer T, Oort FV (2014) Higher temperature sensitivity for stable than for labile soil organic carbon–Evidence from incubations of long-term bare fallow soils. Global Change Biology 20: 633-640. doi: https://doi.org/10.1111/gcb.12402.
29. Li J-Y, Chen P, Li Z-G, Li L-Y, Zhang R-Q, Hu W, Liu Y (2023) Soil aggregate-associated organic carbon mineralization and its driving factors in rhizosphere soil. Soil Biology and Biochemistry 186: 109182. doi: https://doi.org/10.1016/j.soilbio.2023.109182.
30. Li L, Zhang Y, Zhou T, Wang K, Wang C, Wang T, Yuan L, An K, Zhou C, Lü G (2022) Mitigation of China's carbon neutrality to global warming. Nature Communications 13: 5315. doi: https://doi.org/10.1038/s41467-022-33047-9.
31. Liang H, Fu L, Chen H, Zhou G, Gao S, Cao W (2023) Green manuring facilitates bacterial community dispersal across different compartments of subsequent tobacco. Journal of Integrative Agriculture 22: 1199-1215. doi: http://dx.doi.org/10.1016/j.jia.2022.08.043.
32. Liu D, Liu G, Chen L, Wang J, Zhang L (2018a) Soil pH determines fungal diversity along an elevation gradient in Southwestern China. Science China (Life Sciences) 61: 718-726. doi: https://doi.org/10.1007/s11427-017-9200-1.
33. Liu J, Chen X, Zhang J, Xu C, Cao W (2013) Study on characteristics of decomposition and nutrients release of winter green manure crop *Orychophragmus violaceus* in north China. Chinese journal of grassland 35: 58-63 (in Chinese with English abstract).

34. Liu J, Zhang J, Xu C, Bai J, Cao W (2014) Effects of different application rates of *Orychophragmus violaceus* on soil fertility. Agricultural research in the arid areas 32: 123-127 (in Chinese with English abstract).
35. Liu Y, Delgado-Baquerizo M, Wang J, Hu H, Yang Z, He J (2018b) New insights into the role of microbial community composition in driving soil respiration rates. Soil Biology and Biochemistry 118: 35-41. doi: https://doi.org/10.1016/j.soilbio.2017.12.003.
36. Magoč T, Salzberg SL (2011) FLASH: fast length adjustment of short reads to improve genome assemblies. Bioinformatics (Oxford, England) 27: 2957-2963. doi: https://doi.org/10.1093/bioinformatics/btr507.
37. Mancinelli R, Marinari S, Di Felice V, Savin MC, Campiglia E (2013) Soil property, CO2 emission and aridity index as agroecological indicators to assess the mineralization of cover crop green manure in a Mediterranean environment. Ecological Indicators 34: 31-40. doi: https://doi.org/10.1016/j.ecolind.2013.04.011.
38. Mueller ND, Gerber JS, Johnston M, Ray DK, Ramankutty N, Foley JA (2012) Closing yield gaps through nutrient and water management. Nature 490: 254-257. doi: https://doi.org/10.1038/nature11420.
39. Muhammad I, Lv JZ, Wang J, Ahmad S, Farooq S, Ali S, Zhou XB (2022) Regulation of Soil Microbial Community Structure and Biomass to Mitigate Soil Greenhouse Gas Emission. Frontiers in Microbiology 13: 868862. doi: https://doi.org/10.3389/fmicb.2022.868862.
40. Olk DC, Brunetti G, Senesi N (2000) Decrease in Humification of Organic Matter with Intensified Lowland Rice Cropping A Wet Chemical and Spectroscopic Investigation. Soil Science Society of America Journal 64: 1337-1347. doi: https://doi.org/10.2136/sssaj2000.6441337x.
41. Rui Z, Lu X, Li Z, Lin Z, Lu H, Zhang D, Shen S, Liu X, Zheng J, Drosos M, Cheng K, Bian R, Zhang X, Li L, Pan G (2022) Macroaggregates Serve as Micro-Hotspots Enriched With Functional and Networked Microbial Communities and Enhanced Under Organic/Inorganic Fertilization in a Paddy Topsoil From Southeastern China. Frontiers in Microbiology 13: 831746. doi: https://doi.org/10.3389/fmicb.2022.831746.
42. Saiya-Cork KR, Sinsabaugh RL, Zak DR (2002) The effects of long term nitrogen deposition on extracellular enzyme activity in an Acer saccharum forest soil. Soil Biology Biochemistry 34: 1309-1315. doi: https://doi.org/10.1016/S0038-0717(02)00074-3.
43. Sinsabaugh RL, Gallo ME, Lauber C, Waldrop MP, Zak DR (2005) Extracellular Enzyme Activities and Soil Organic Matter Dynamics for Northern Hardwood Forests receiving Simulated Nitrogen Deposition. Biogeochemistry 75: 201-215. doi: https://doi.org/10.1007/s10533-004-7112-1.
44. Tapia-Vázquez I, Sánchez-Cruz R, Arroyo-Domínguez M, Lira-Ruan V, Sánchez-Reyes A, del Rayo Sánchez-Carbente M, Padilla-Chacón D, Batista-García RA, Folch-Mallol JL (2020) Isolation and characterization of psychrophilic and psychrotolerant plant-growth promoting microorganisms from a high-altitude volcano crater in Mexico. Microbiological Research 232: 126394. doi: https://doi.org/10.1016/j.micres.2019.126394.

45. Team RC (2012) R: A Language And Environment For Statistical Computing. R Foundation for Statistical Computing: Vienna, Austria. http://www.R-project.org.
46. Tringe S, von Mering C, Kobayashi A, Salamov A, Chen K, Chang H, Podar M, Short J, Mathur E, Detter J, Bork P, Philip H, Rubin E (2005) Comparative Metagenomics of Microbial Communities. Science (New York, NY) 308: 554-557. doi: https://doi.org/10.1126/science.1107851.
47. Trinsoutrot I, Recous S, Bentz B, Linères M, Chèneby D, Nicolardot B (2000) Biochemical Quality of Crop Residues and Carbon and Nitrogen Mineralization Kinetics under Nonlimiting Nitrogen Conditions. Soil Science Society of America Journal 64: 918-926. doi: https://doi.org/10.2136/sssaj2000.643918x.
48. Trivedi P, Rochester IJ, Trivedi C, Van Nostrand JD, Zhou J, Karunaratne S, Anderson IC, Singh BK (2015) Soil aggregate size mediates the impacts of cropping regimes on soil carbon and microbial communities. Soil Biology and Biochemistry 91: 169-181. doi: https://doi.org/10.1016/j.soilbio.2015.08.034.
49. Vance ED, Brookes PC, Jenkinson DS (1987) An extraction method for measuring soil microbial biomass C. Soil Biology Biochemistry 19: 703-707. doi: https://doi.org/10.1016/0038-0717(87)90052-6.
50. Virk AL, Lin B, Kan Z, Qi J, Dang YP, Lal R, Zhao X, Zhang H (2022) Chapter Two-Simultaneous effects of legume cultivation on carbon and nitrogen accumulation in soil. In: DL Sparks (ed) Advances in Agronomy. Academic Press.
51. Wan S, Shan S, Guo F (2010) Improving Peanut Production Capacity to Ensure Oil Supply. Journal of Agricultural Science and Technology 12: 22-26 (in Chinese with English abstract).
52. Wang Y, Liu K, Zhou Y, Chen Y, Jin C, Hu Y (2023) Integrated Analysis of microRNA and RNA-Seq Reveals Phenolic Acid Secretion Metabolism in Continuous Cropping of Polygonatum odoratum. Plants 12: 943. doi: https://doi.org/10.1186/s12864-017-3995-9.
53. West JR, Lauer JG, Whitman T (2023) Tillage homogenizes soil bacterial communities in microaggregate fractions by facilitating dispersal. Soil Biology and Biochemistry 186: 109181. doi: https://doi.org/10.1016/j.soilbio.2023.109181.
54. Wilhelm RC, Amsili JP, Kurtz KSM, van Es HM, Buckley DH (2023) Ecological insights into soil health according to the genomic traits and environment-wide associations of bacteria in agricultural soils. ISME Communications 3: 1. doi: https://doi.org/10.1038/s43705-022-00209-1.
55. Wu A, Jiao X, Wang J, Dong E, Guo J, Wang L, Sun A, Hu H (2021) Sorghum rhizosphere effects reduced soil bacterial diversity by recruiting specific bacterial species under low nitrogen stress. Science of The Total Environment 770: 144742. doi: https://doi.org/10.1016/j.scitotenv.2020.144742.
56. Wu Z, Tang Z, Yu T, Zhang J, Zheng Y, Yang J, Wu Y, Sun Q (2023a) Nitrogen fertilization rates mediate rhizosphere soil carbon emissions of continuous peanut monoculture by altering cellulose-specific microbes. Frontier in Plant Science 14: 1109860. doi: https://doi.org/10.3389/fpls.2023.1109860.

57. Wu Z, Zheng Y, Sui X, Zhang Z, Wang E, Liu Y, Yu T, Yang J, Wu Y (2023b) Comparative analysis of the effects of conventional and biodegradable plastic mulching films on soil-peanut ecology and soil pollution. Chemosphere 334: 139044. doi: https://doi.org/10.1016/j.chemosphere.2023.139044.
58. Xie X, Zhang H, Pare P (2009) Sustained growth promotion in Arabidopsis with long-term exposure to the beneficial soil bacterium Bacillus subtilis (GB03). Plant Signaling & Behavior 4: 948-953. doi: https://doi.org/10.4161/psb.4.10.9709.
59. Xu M, Qi Y (2001) Spatial and seasonal variations of Q_{10} determined by soil respiration measurements at a Sierra Nevadan Forest. Global Biogeochemical Cycles 15: 687-696. doi: https://doi.org/10.1029/2000gb001365.
60. Xu Y, Ding H, Zhang G, Li Z, Guo Q, Feng H, Qin F, Dai L, Zhang Z (2023) Green manure increases peanut production by shaping the rhizosphere bacterial community and regulating soil metabolites under continuous peanut production systems. BMC Plant Biology 23: 69. doi: https://doi.org/10.1186/s12870-023-04079-0.
61. Yan M, Zhou X, Liu Z, Zhang Y (2023a) Study on the pattern and contributing factors of increasing production of vegetable oil crops in China. China Oils and Fats. doi: https://doi.org/10.19902/j.cnki.zgyz.1003-7969.230054 (in Chinese with English abstract).
62. Yan Z, Zhou J, Liu C, Jia R, Mganga KZ, Yang L, Yang Y, Peixoto L, Zang H, Zeng Z (2023b) Legume-based crop diversification reinforces soil health and carbon storage driven by microbial biomass and aggregates. Soil and Tillage Research 234: 105848. doi: https://doi.org/10.1016/j.still.2023.105848.
63. Yim B, Ibrahim Z, Rüger L, Ganther M, Maccario L, Sørensen SJ, Heintz-Buschart A, Tarkka MT, Vetterlein D, Bonkowski M, Blagodatskaya E, Smalla K (2022) Soil texture is a stronger driver of the maize rhizosphere microbiome and extracellular enzyme activities than soil depth or the presence of root hairs. Plant and Soil 478: 229-251. doi: https://doi.org/10.1007/s11104-022-05618-8.
64. Zeng J, Liu X, Song L, Lin X, Zhang H, Shen C, Chu H (2016) Nitrogen fertilization directly affects soil bacterial diversity and indirectly affects bacterial community composition. Soil Biology and Biochemistry 92: 41-49. doi: https://doi.org/10.1016/j.soilbio.2015.09.018.
65. Zhang X, Zhang R, Gao J, Wang X, Fan F, Ma X, Yin H, Zhang C, Feng K, Deng Y (2017) Thirty-one years of rice-rice-green manure rotations shape the rhizosphere microbial community and enrich beneficial bacteria. Soil Biology and Biochemistry 104: 208-217. doi: https://doi.org/10.1016/j.soilbio.2016.10.023.
66. Zhang Z, An J, Han Y, Feng L, Li X, Xiong S, Xing F, Xin M, Li Y, Wang Z (2021) Advantages of an Orychophragmus violaceus-maize rotation in reducing greenhouse gas emissions and reactive nitrogen losses and increasing net ecosystem economic benefits on the North China Plain. Journal of Cleaner Production 317: 128426. doi: https://doi.org/10.1016/j.jclepro.2021.128426.
67. Zhang Z, Li X, Xiong S, an J, Han Y, Wang G, Feng L, Lei Y, Yang B, Xing F, Xin M, Du W, Wang Z, Li Y (2022) Orychophragmus violaceus as a winter cover crop is more conducive to agricultural

sustainability than Vicia villosa in cotton-fallow systems. Archives of Agronomy and Soil Science 68: 1487-1500. doi: https://doi.org/10.1080/03650340.2021.1905800.

68. Zhao M, Ma T, Zhao J, Deng K, Xiao Y, Ma J, Mao J, Jia P, Diao Q (2017) Determination and Estimation of Available Energy Value of Peanut Vine as Single Straw Feed for Mutton Sheep. Chinese Journal of Animal Nutrition 29: 4162-4170 (In Chinese).
69. Zhao Q, Gao X, Wu D, Cao W (2010) Salt tolerance of winter green manure Orychophragmus violaeeus and its fertilizer effect in the saline-alkali arable land. Soil and Fertilizer in China 4: 65-68 (in Chinese with English abstract).
70. Zhou G, Cao W, Bai J, Xu C, Zeng N, Gao S, Rees RM, Dou F (2020) Co-incorporation of rice straw and leguminous green manure can increase soil available nitrogen (N) and reduce carbon and N losses: An incubation study. Pedosphere 30: 661-670. doi: https://doi.org/10.1016/S1002-0160(19)60845-3.

Figures

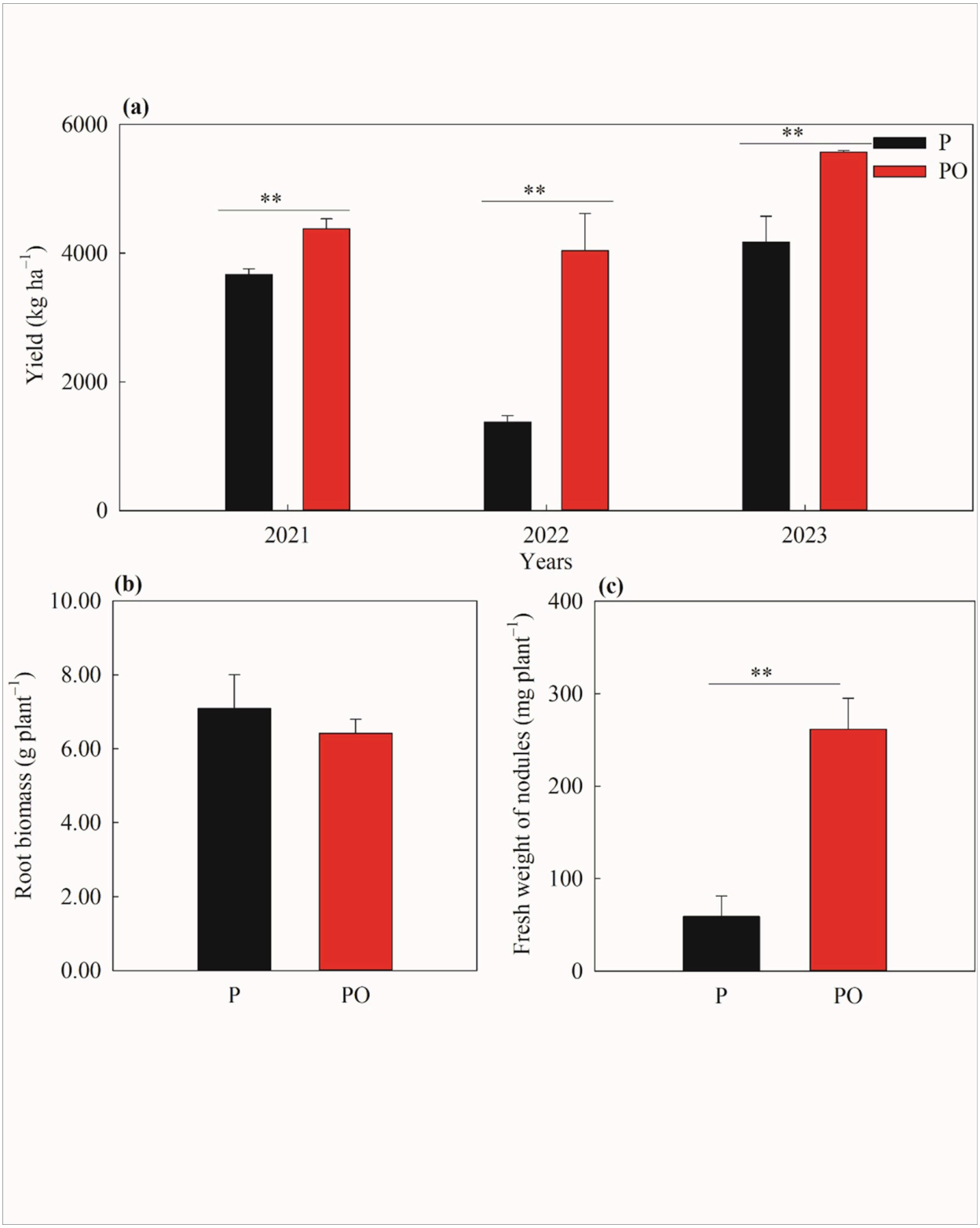

Figure 1

Peanut yields from 2021 to 2023 (a.), root biomass (b.) and fresh weight of nodules in 2023 (c.). Asterisks represent significant differences between the P and PO treatments at $P<0.05$. P and PO denote the continuous peanut monoculture and peanut-*O. violaceus* rotation, respectively. Different lowercase letters denote the differences between cropping regimesat $P<0.05$, ANOVA (±SE, $n=3$).

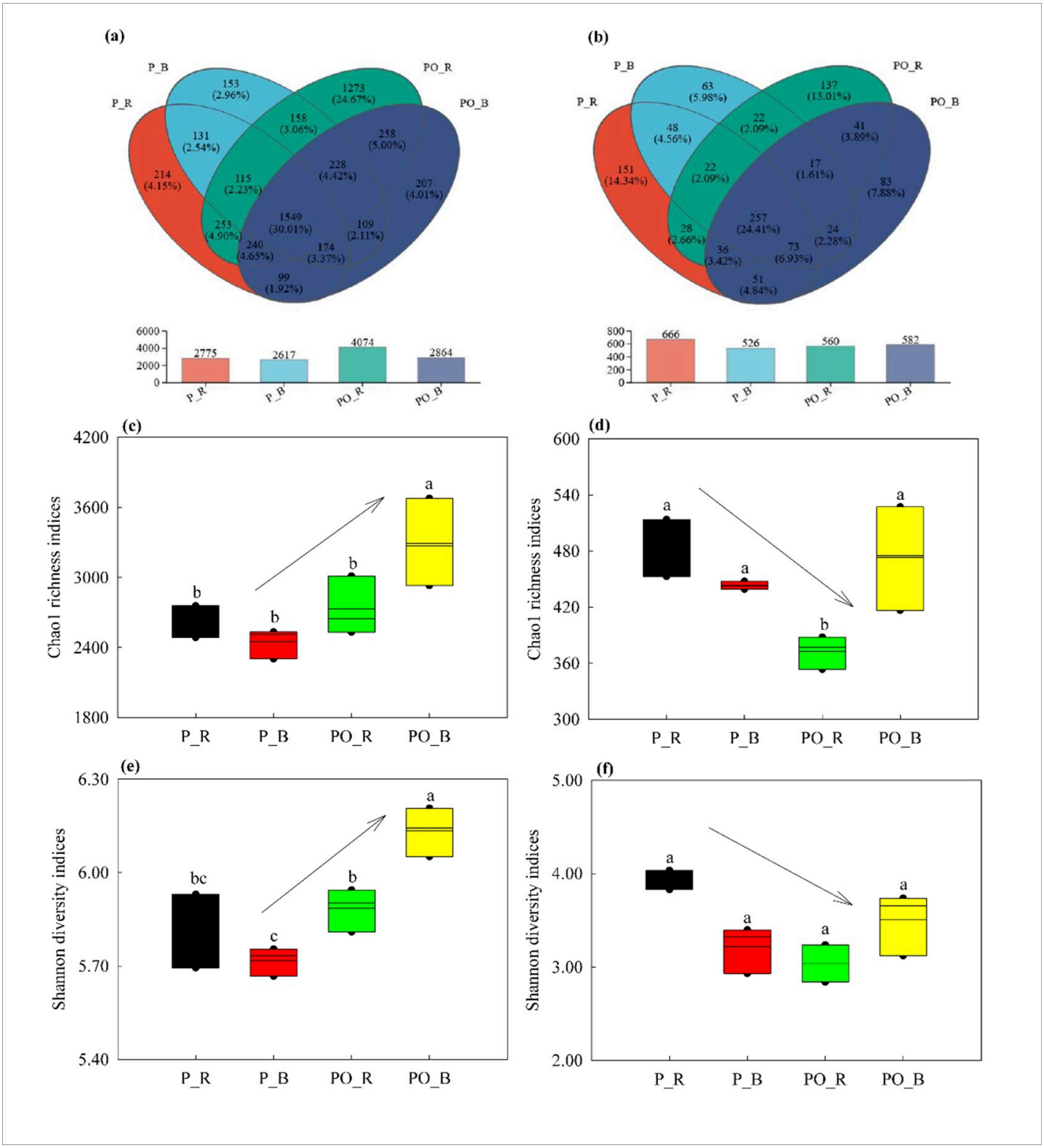

Figure 2

Venn diagrams (a. and b.), Chao1 richness (c. and d.) and Shannon diversity (e. and f.) indices of bacterial and fungal communities. P and PO denote continuous peanut monoculture and peanut-*O. violaceus* rotation, respectively; R and B are short for the rhizosphere and bulk soil, respectively. Different lowercase letters denote the differences between crop regimes at $P<0.05$, ANOVA (±SE, $n=3$).

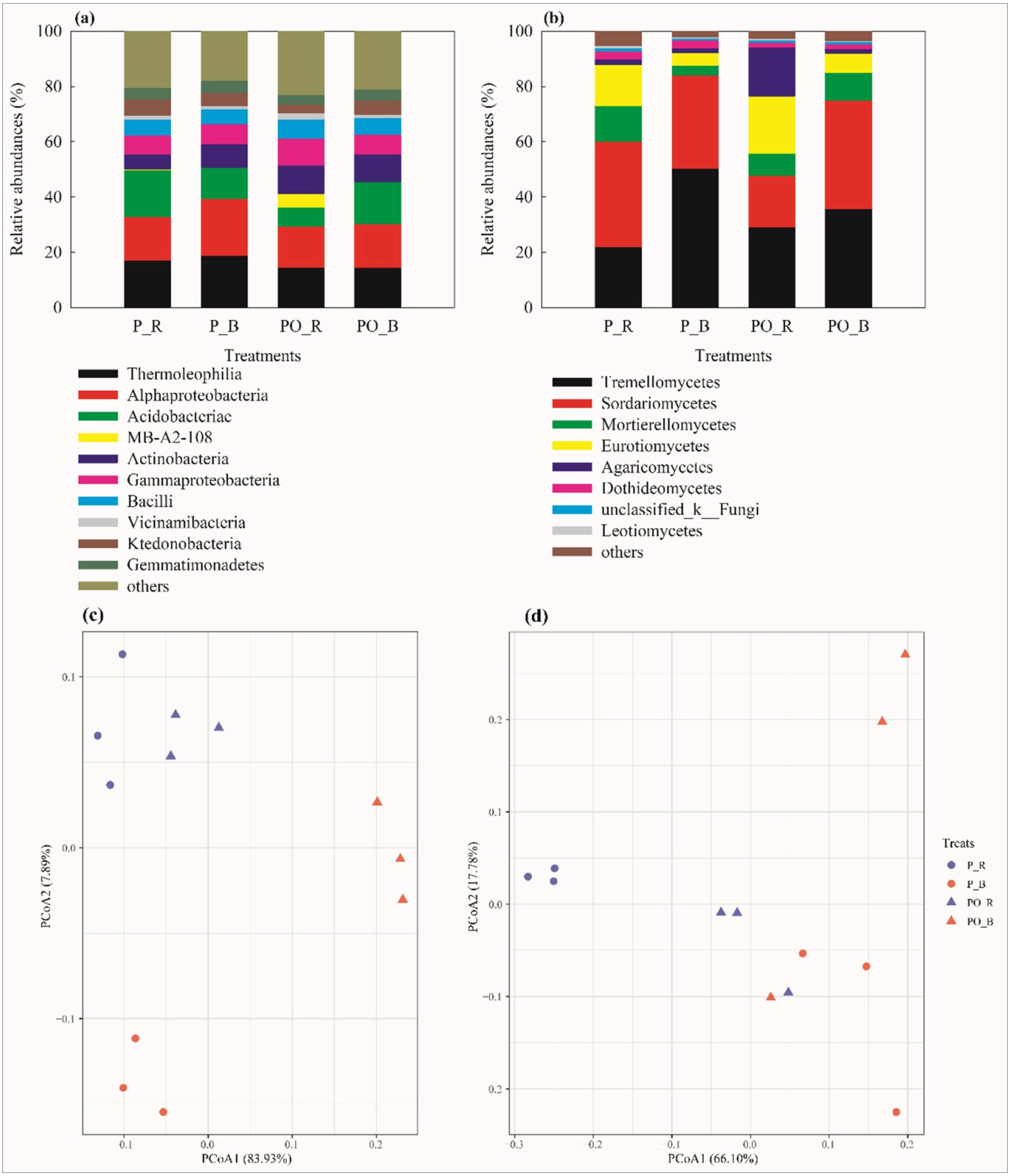

Figure 3

Relative abundances of the dominant bacterial and fungal OTUs at the class level (a. and b.), and PCoA of bacterial and fungal communities (c. and d.) based on the Bray-Curtis distance. P and PO denote continuous peanut monoculture and peanut-*O. violaceus* rotation, respectively; R and B are short for the rhizosphere and bulk soil, respectively.

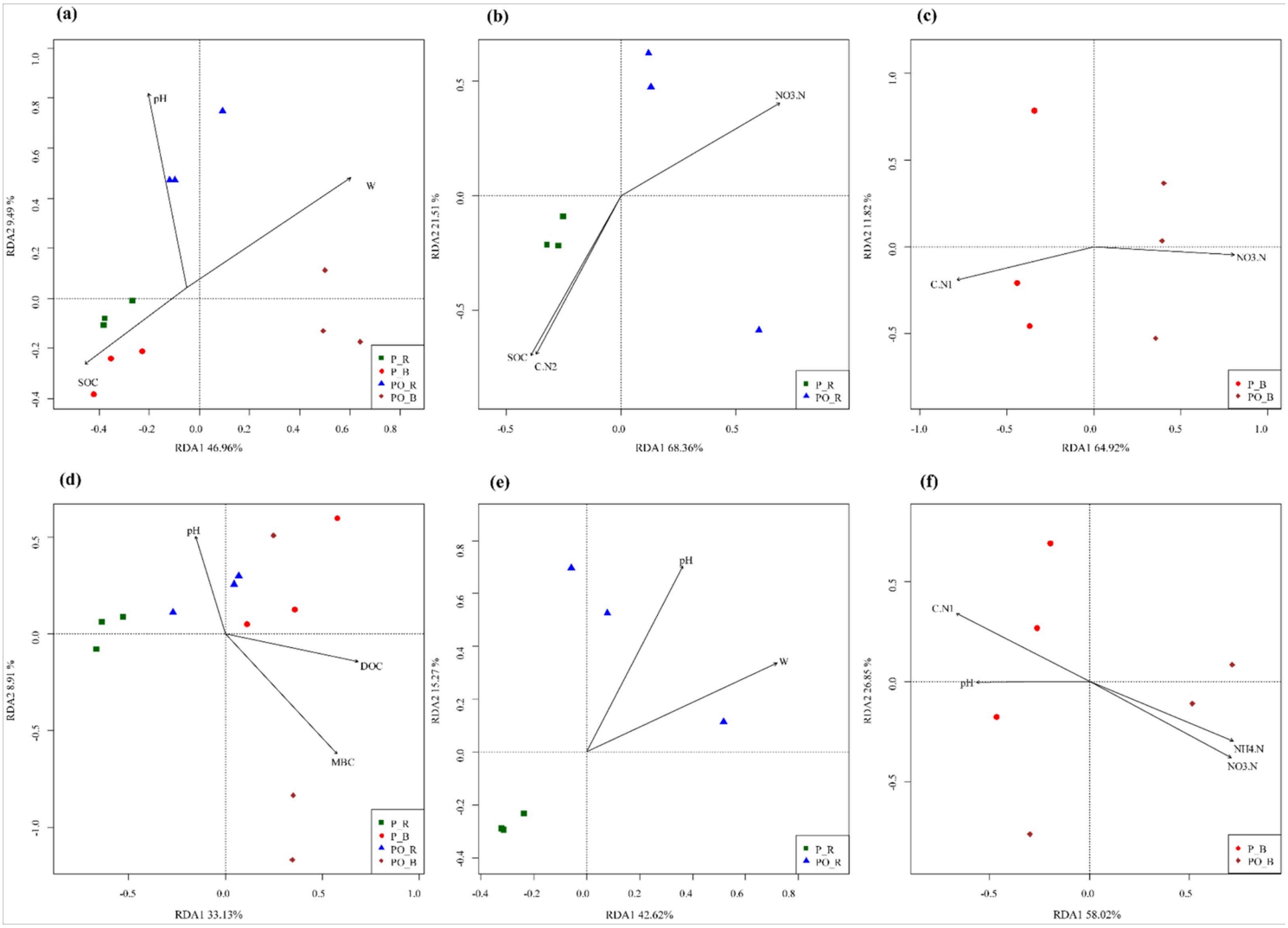

Figure 4

Ordination plots of the redundancy analysis to identify relationships between the bacterial (a, b and c) and fungal (d, e and f) OTUs and environmental variables for all samples, rhizosphere samples and bulk soil samples, respectively. W, soil water content; SOC, soil total organic carbon; DOC, dissolved organic carbon; N_{min}, soil mineral nitrogen; C/N1, soil dissolved carbon: mineral nitrogen ratio; C/N2, soil total organic carbon content: total nitrogen ratio. P and PO denote the continuous peanut monoculture and peanut-*O. violaceus* rotation, respectively; R and B are short for the rhizosphere and bulk soil, respectively.

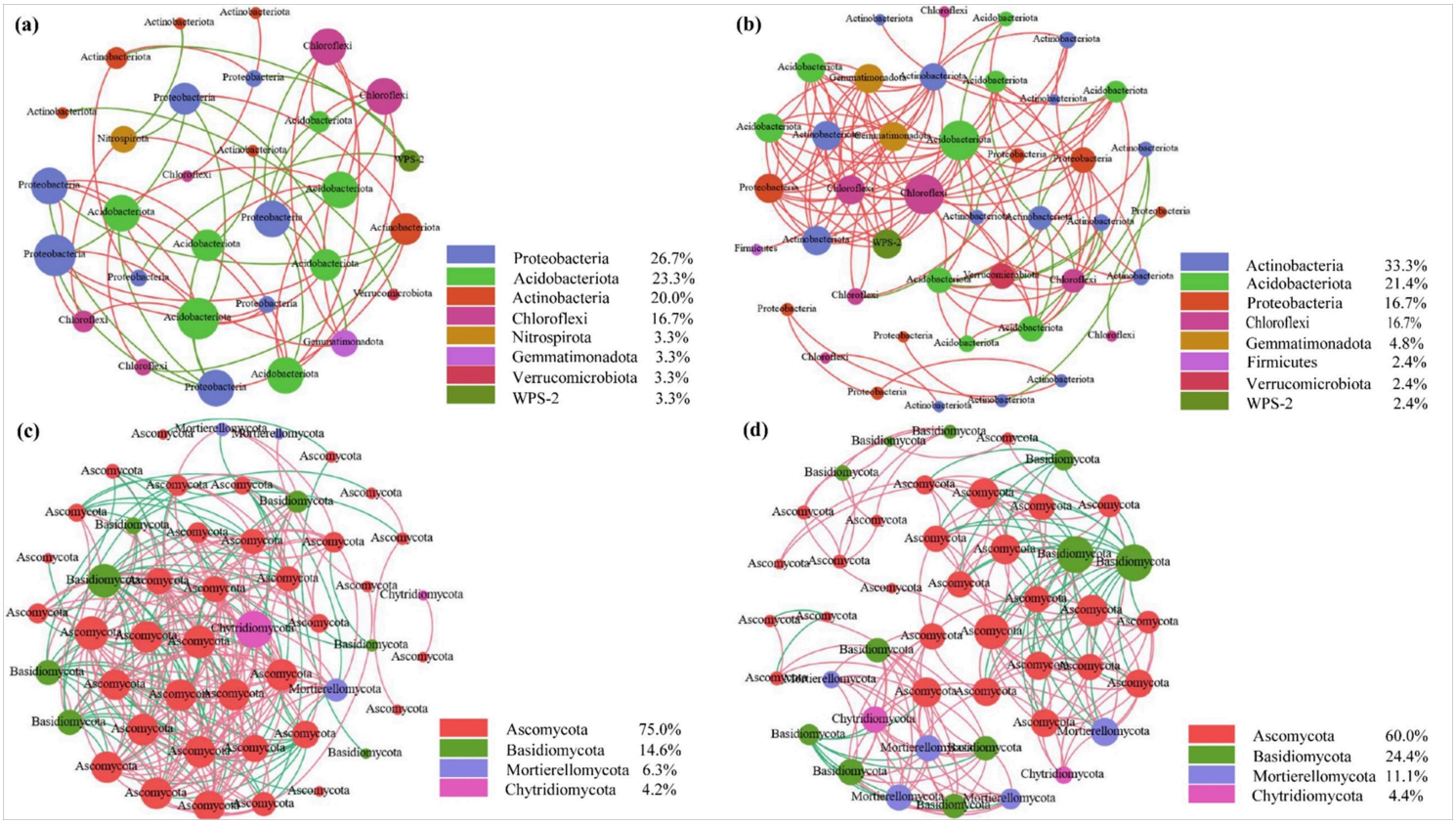

Figure 5

Bacterial and fungal co-occurrence networks of P (A. and B.) and PO (C. and D.). A connection denotes a significant correlation (Pearson's ρ>0.70, *P*<0.05), and a node represents an operational taxonomic unit (97% sequence identity threshold, OTUs). The size of each node is proportional to the degree of connectivity, and the thickness of each connection between two nodes is proportional to the values of Pearson's correlation coefficient. P and PO denote continuous peanut monoculture and peanut-*O. violaceus* rotation, respectively.

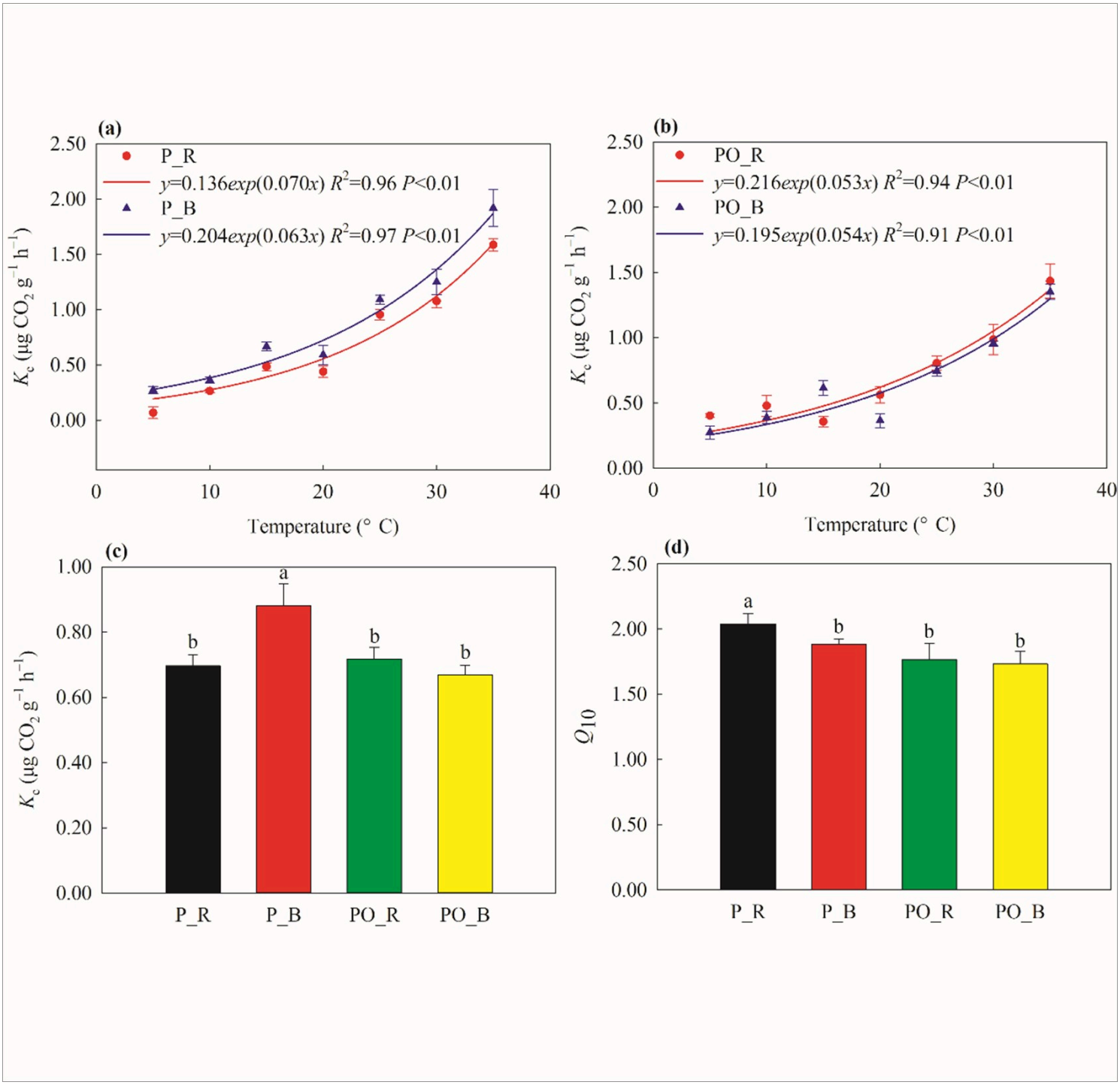

Figure 6

Figure 6 The exponential growth curves between the SOC decomposition rates (K_c) and the incubation temperature for the rhizosphere and bulk soil of P (a.) and PO (b.), and the average K_c (c.) and Q_{10} values (d.) (n=3). P and PO denote continuous peanut monoculture and peanut-*O. violaceus* rotation, respectively; R and B are short for the rhizosphere and bulk soil, respectively.

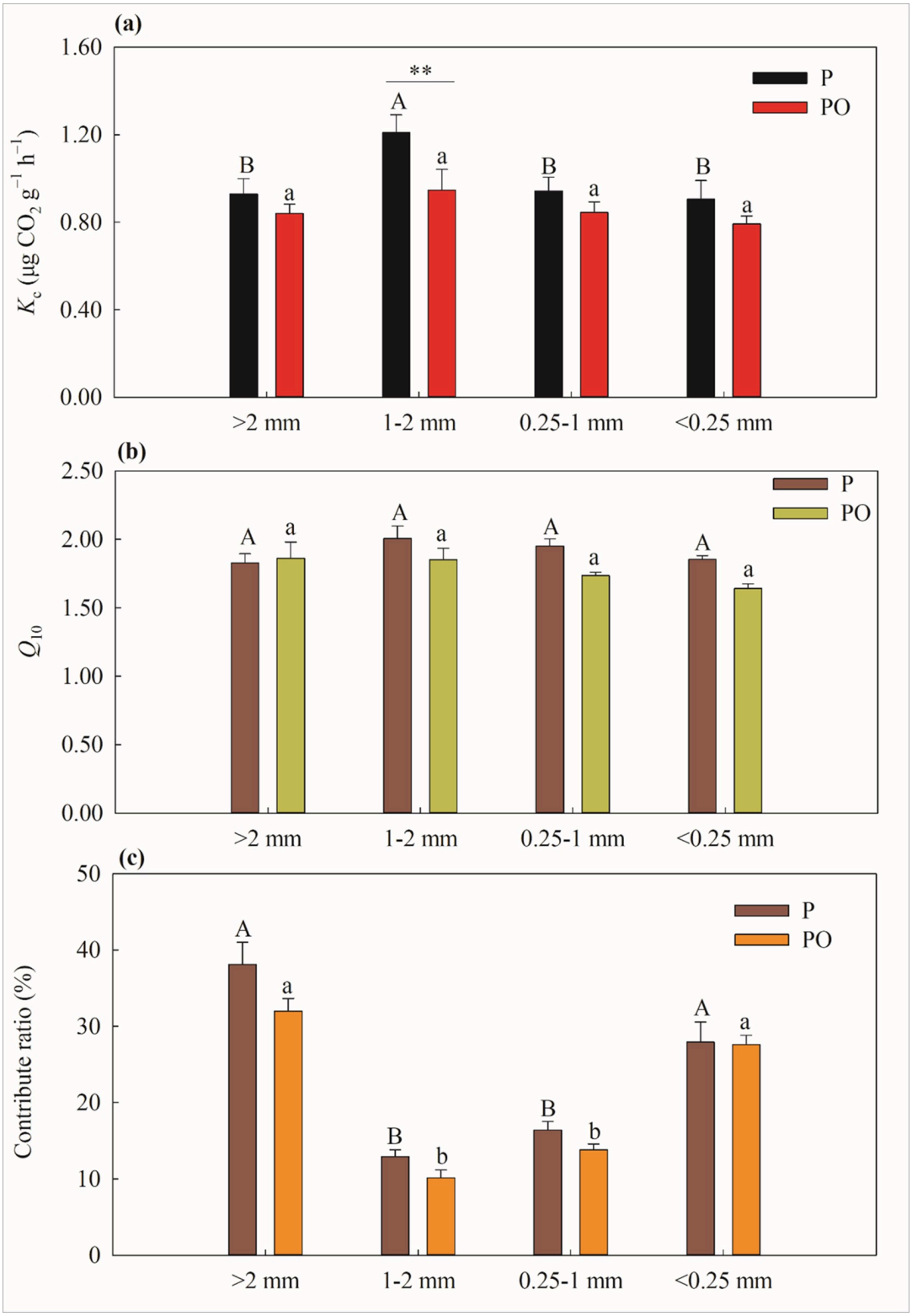

Figure 7

The averaged SOC decomposition rates (a. K_c), Q_{10} values (b.) for the bulk soil aggregates and the contribution ratio of each size of aggregate to K_c (c.) of the two treatments (n=3). The capital letters denote the differences among aggregates of the P treatment, and the lowercase letters denote the differences among aggregates of the PO treatments. P and PO denote continuous peanut monoculture

and peanut-*O. violaceus* rotation, respectively. Asterisks represent significant differences between the P and PO treatments at $P<0.05$.

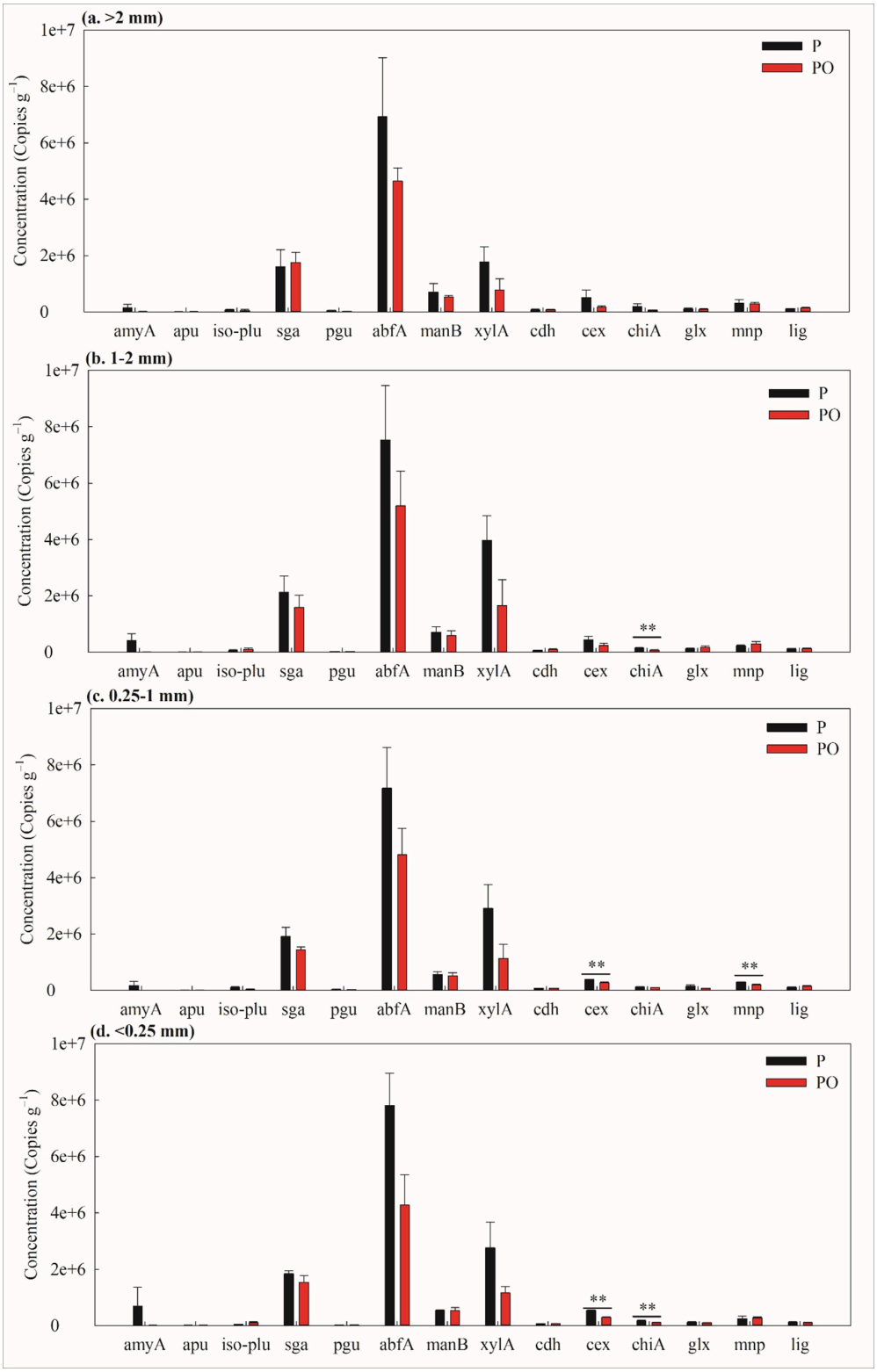

Figure 8

Functional genes involved in carbon degradation of each aggregate (a: >2 mm; b: 1–2 mm; c: 0.25–1 mm and d: <0.25 mm aggregates) from the soil of the two treatments. The capital letters denote the differences between aggregates of the P treatment, and the lowercase letters denote the differences

between aggregates of the PO treatments. P and PO denote continuous peanut monoculture and peanut-*O. violaceus* rotation, respectively. Asterisks represent significant differences between the P and PO treatments at $P<0.05$.

Supplementary Files

This is a list of supplementary files associated with this preprint. Click to download.

- Supplementarytablesfigures.docx